Mechanics of soft composites:

From deployable structures to self-organized patterns

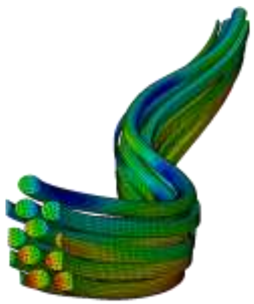 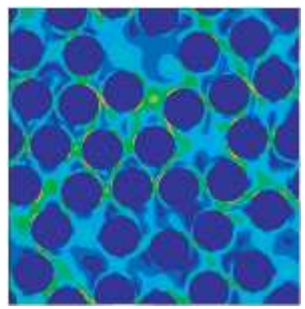 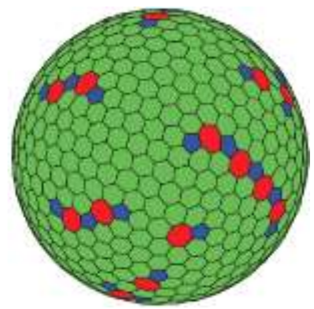 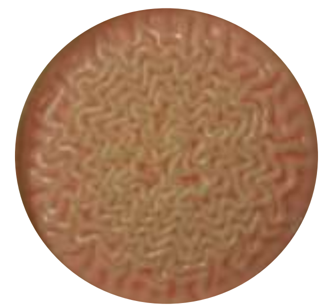

Francisco Lopez Jimenez

Ecole Polytechnique Federale de Lausanne
Institute of Mechanical Engineering
Feb 2nd 2016

Structures traditionally seen as a system of connected parts with the goal of bearing a load while maintaining shape.

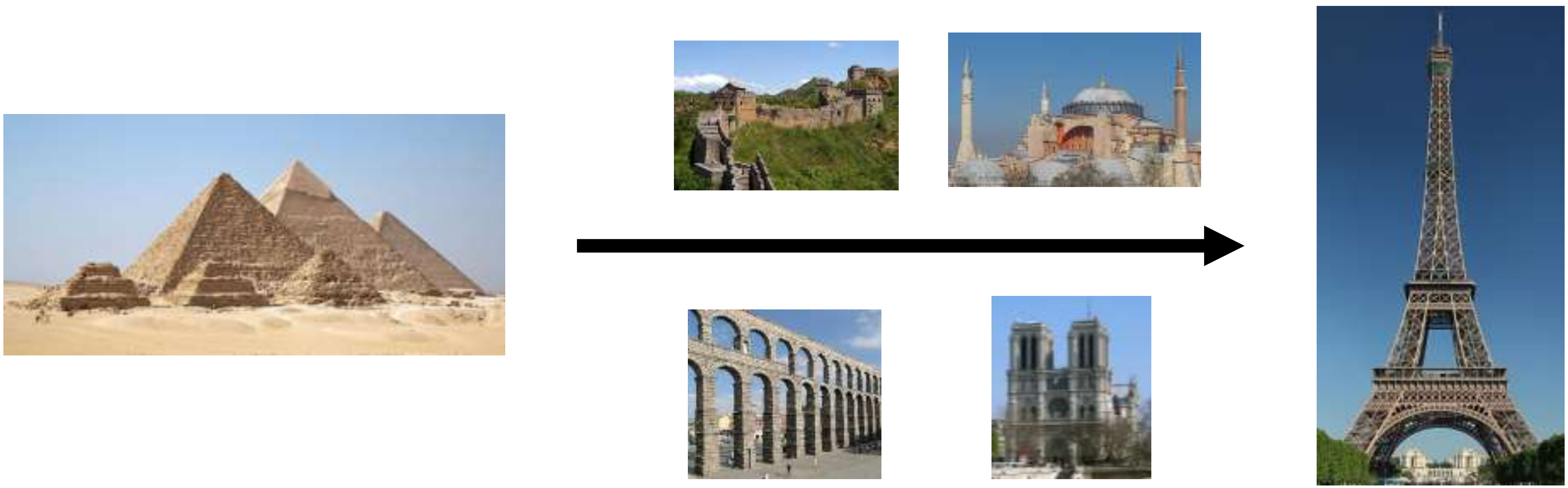

Structural mechanics applied now much more widely.

Materials with engineered microstructure


Macro

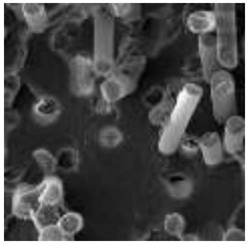
Micro

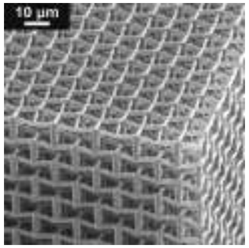

Nano

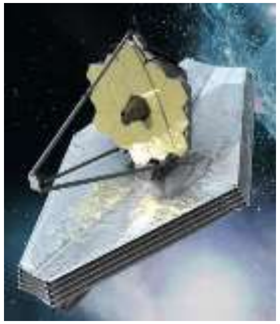

The line between material and structure is no longer clear.

Structures now make use of the nonlinear regime

Flexible | Active | Multiphysics

Harnessing instabilities | Biological systems

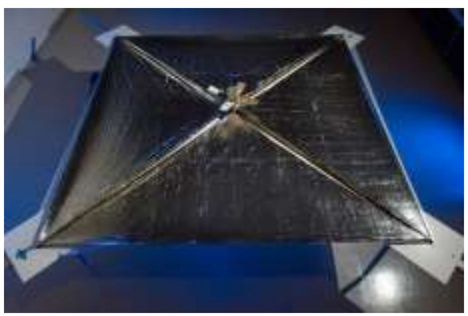

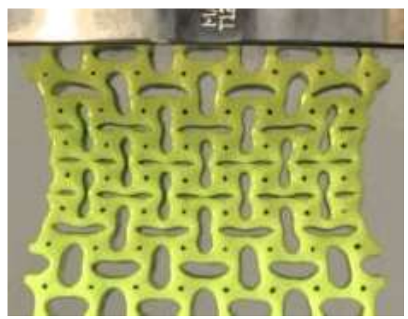

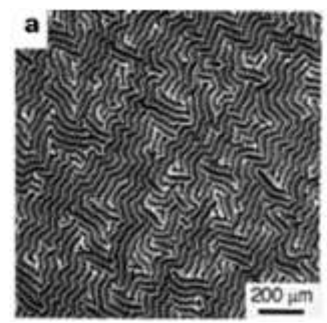

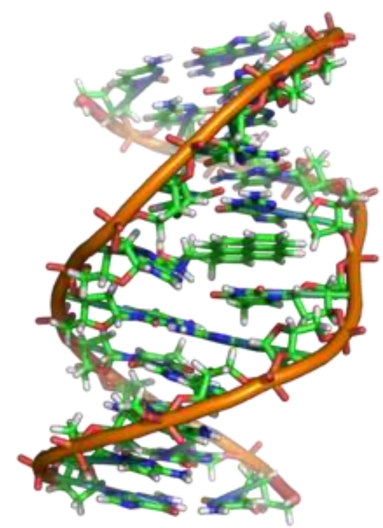

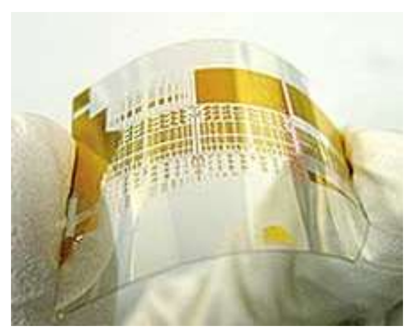

Materials with engineered microstructure + **Nonlinear mechanics of soft solids**

Cellular solids

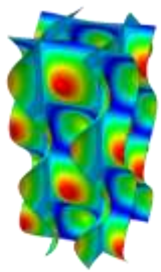
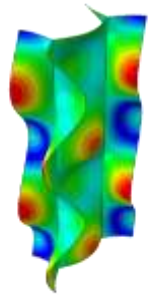

Flexible fiber composites

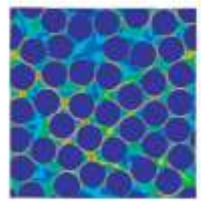

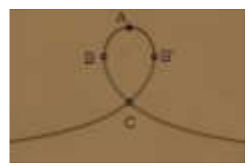

Patterns on soft solids


Granular media

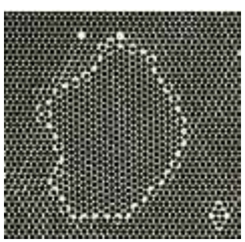

Textiles

Materials optical attenuation

FLEXIBLE FIBER COMPOSITES

Collaboration with:

Prof. Sergio Pellegrino (Caltech)

Dr. Juan Mejia-Ariza (L'Garde)

Prof. Oscar Lopez-Pamies (UIUC)

MOTIVATION

Deployable methods, especially for precision large rigid structures or <u>flexible materials</u> are the enabling force behind developing the larger systems needed to attain advancements in science and engineering of today and tomorrow.

NASA Space Technology Roadmap, 2012

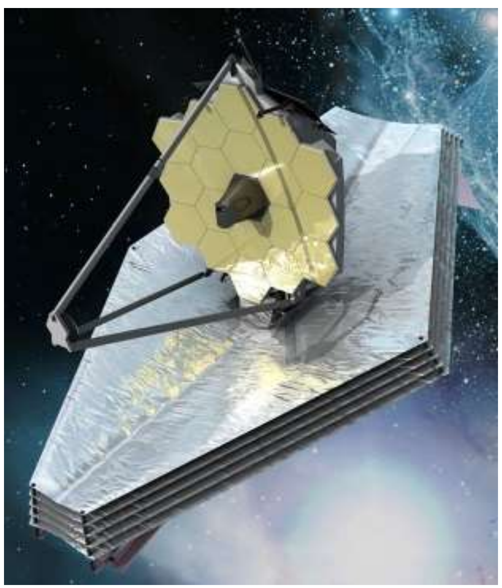

James Webb
Space Telescope

Sun shield (12.2 m × 18 m)

MOTIVATION

Traditional deployable structures are rigid and require mechanical elements:

- Complex
- Heavy
- Expensive
- External actuation

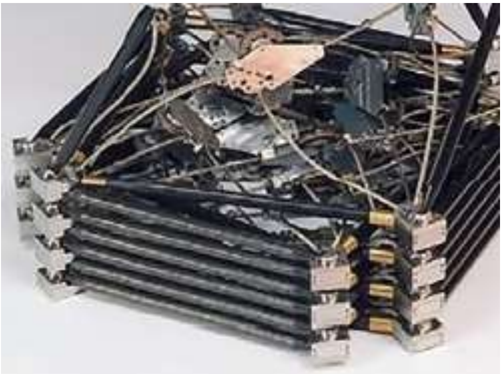

Folded mast (atk.com)

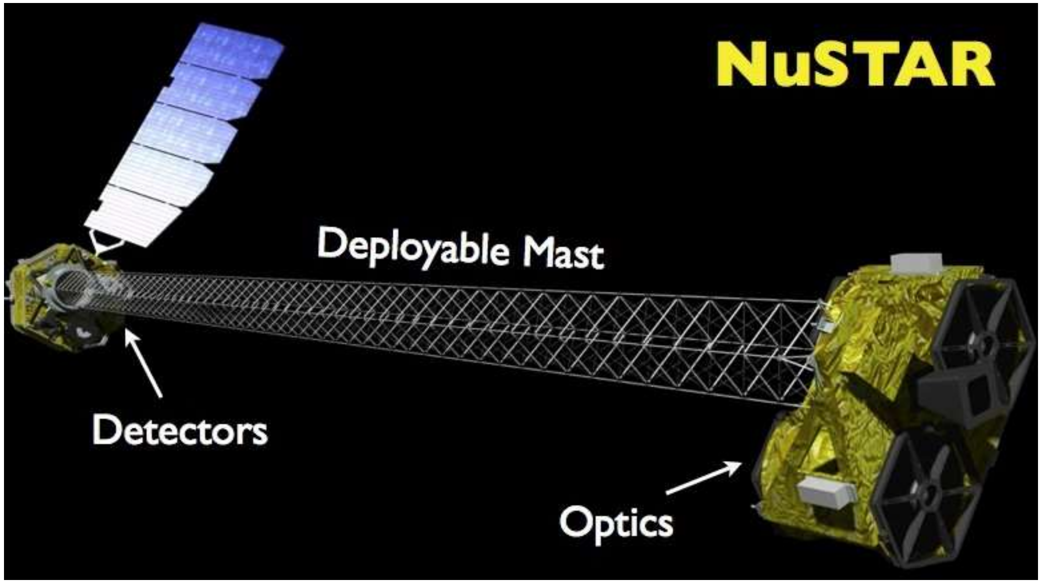

NuSTAR – Space x-ray telescope (caltech.edu)

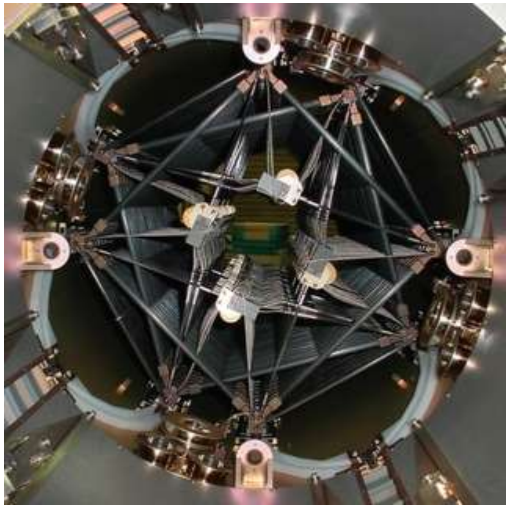

Stowed mast in canister (atk.com)

MOTIVATION

An alternative are structures that deform elastically during packing.

The structure self deploys releasing strain energy.

Designs are limited by the curvature failure of the material.

Northrop Grumman Astro Aerospace Flattenable Foldable Tubes for the Mars Express (Adams et al., 2009)

Boeing reflectors on the Mobile Satellite System (Tan et al., 2006)

DLR-CFRP boom, German Aerospace Center (Leipold et al., 2005)

MOTIVATION

Fiber composites with a very soft elastomeric matrix can be folded to very high curvatures without breaking.

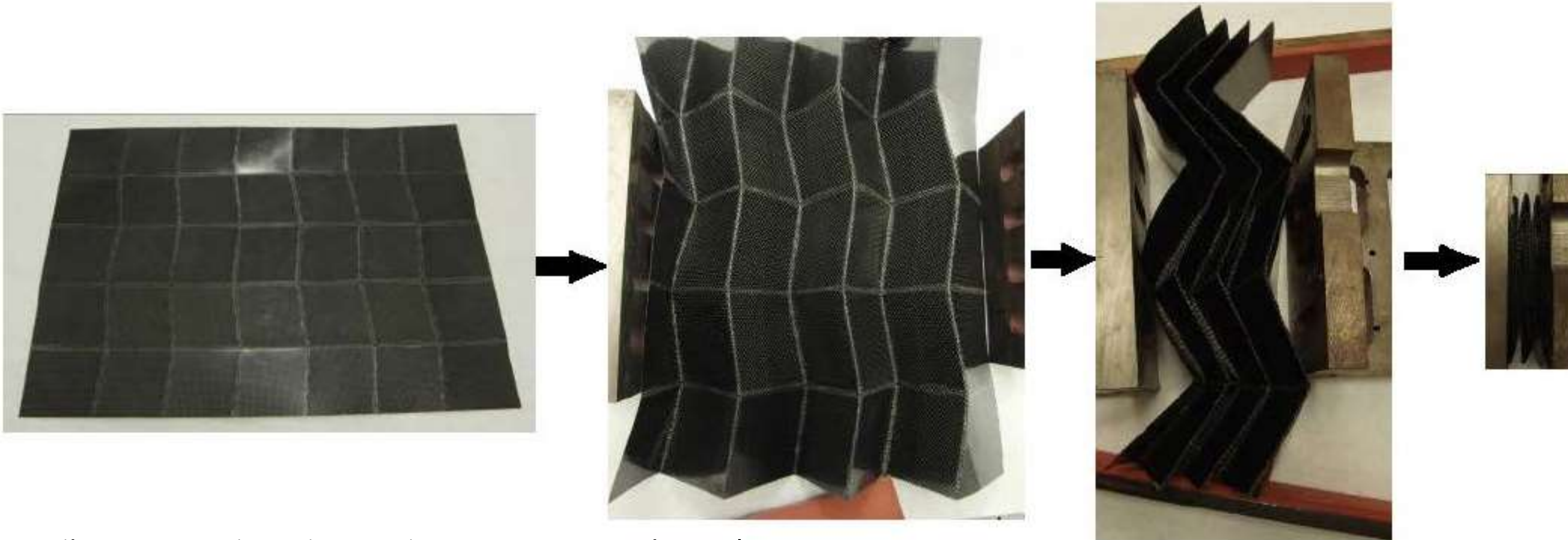

Fiber composite Miura-Ori pattern (Maqueda et al., 2012)

Why does this happen?

Does it have any effect on the material?

How tightly can we pack the composite?

WHY DOES THIS HAPPEN?

When folded, the fibers microbuckle without breaking.

Fiber microbuckling acts as a stress relief mechanism.

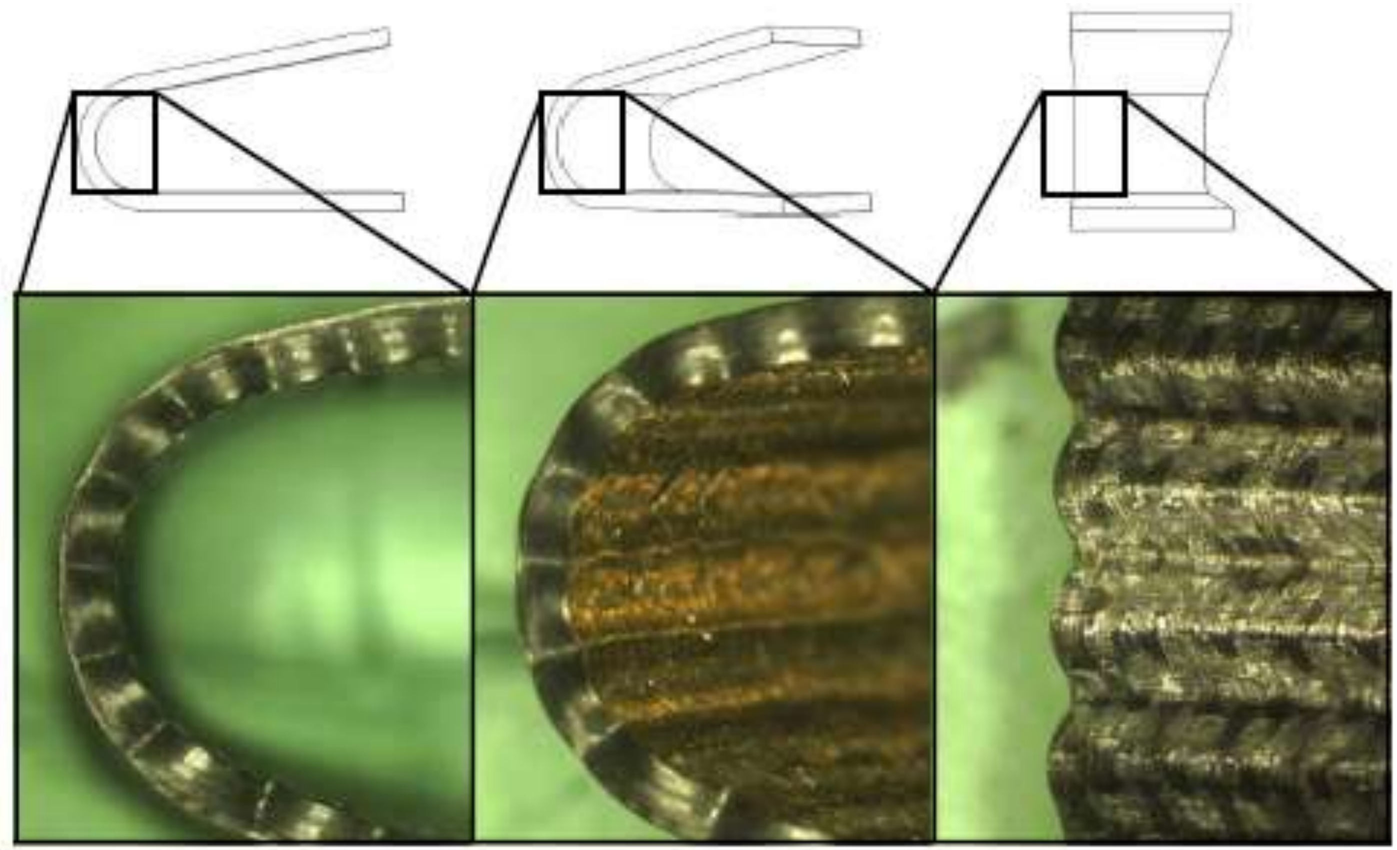

Elastic Memory Composite bent at high temperature (Francis, 2008)

EXPERIMENTAL CHARACTERIZATION

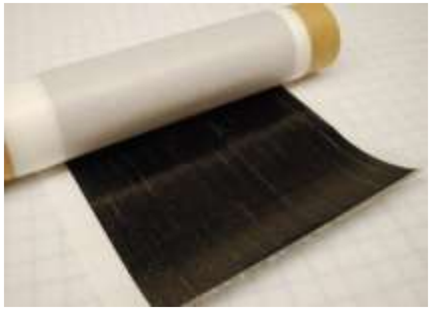

HTS40-12K carbon fibers (TohoTenax)

Diameter: 7 μm

Tensile modulus: 240 GPa

Failure strain: 1.8 %

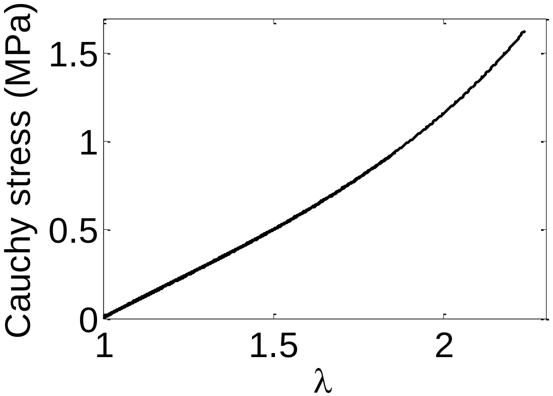

CF19-2615 silicone (NuSil Technology)

Initial tensile modulus: 1 MPa

Failure elongation: 120% – 140%

No viscoelastic behavior or Mullins effect observed.

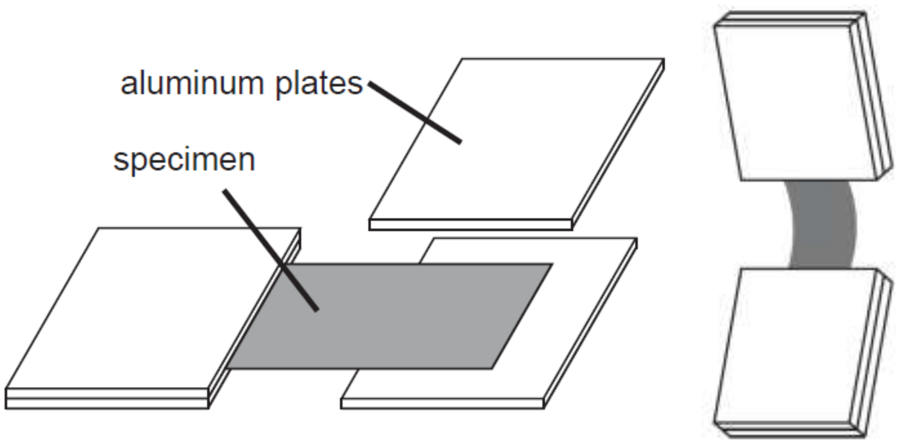

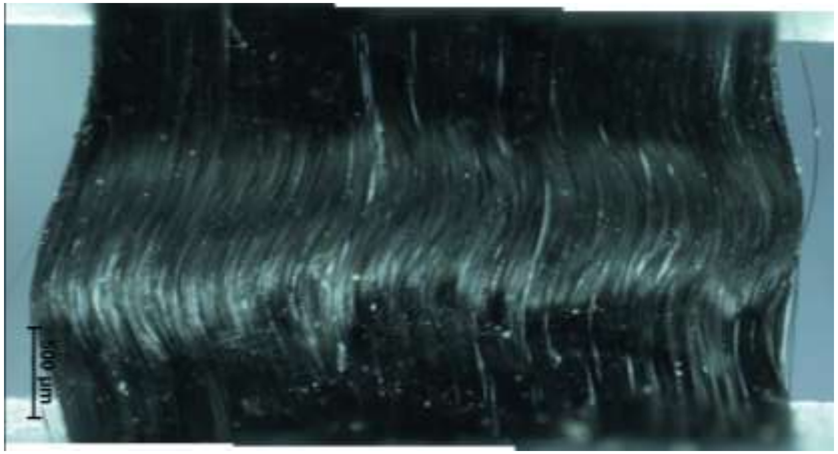

V_f = 30%, κ = 0.5 mm^{-1}

Bending behavior:

- Highly nonlinear
- Strain softening and hysteresis under cyclic loading

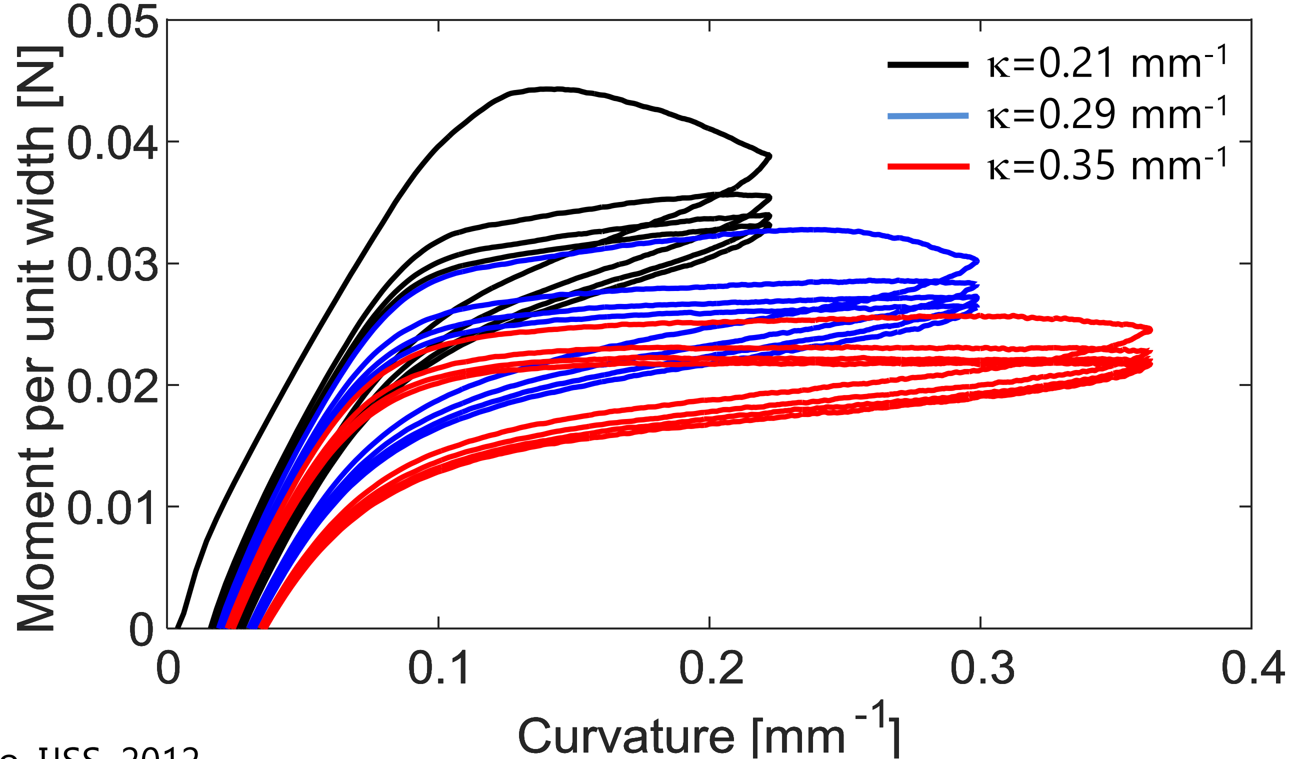

FLJ and Pellegrino, IJSS, 2012

EXPERIMENTAL CHARACTERIZATION

It is hard to decouple material effects from the nonlinearities due to microbuckling.

Tension perpendicular to the fibers isolates the effects of damage.

Behavior close to typical filled rubber (Mullins effect).

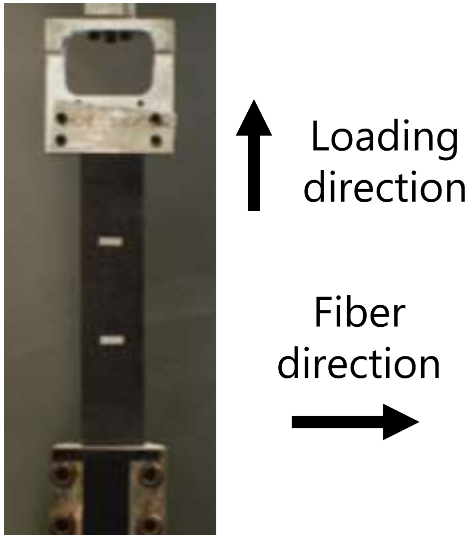

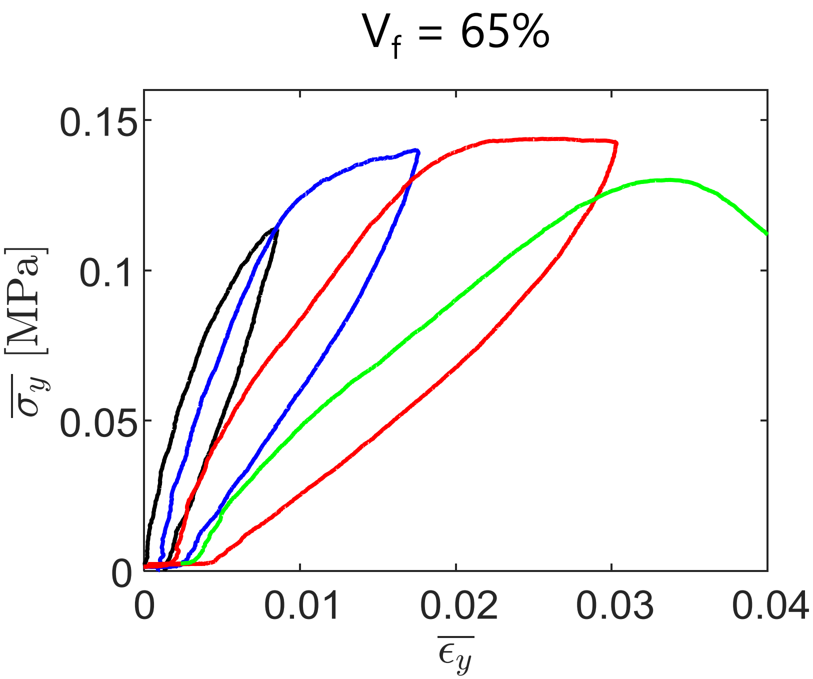

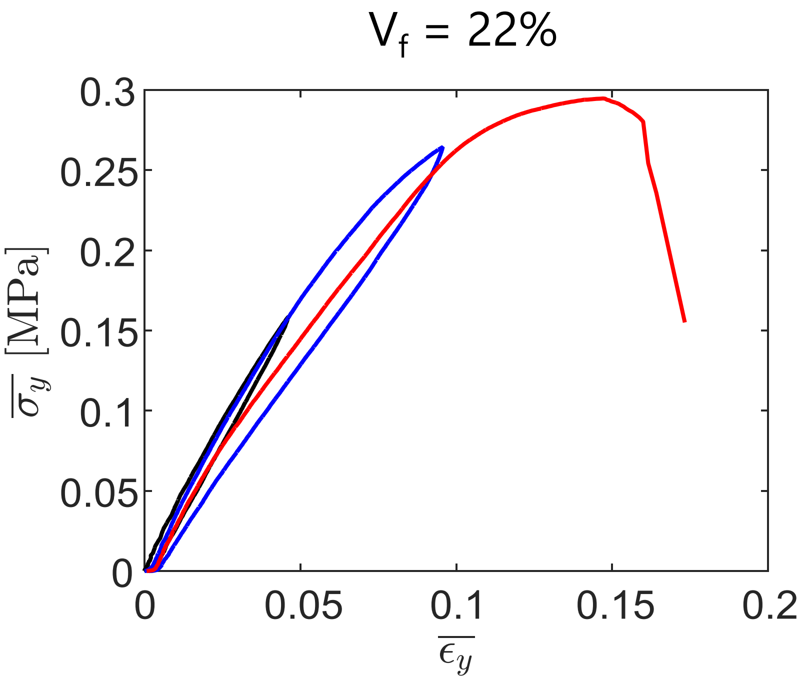

Finite element model in Abaqus/Standard:

- Representative volume element (RVE) with periodic boundary conditions

- Continuum elements used for both fiber and matrix

- Gent hyperelastic model for the matrix, fitted from tensile experiments:

$$W = -C_1 J_m \ln\left(1 - \frac{J_1}{J_m}\right) + C_2 \ln\left(\frac{J_2 + 3}{3}\right)$$

- Different fiber distributions used:
  - Purely random
  - Random based on micrographs

FINITE ELEMENT MODELING

Usual idealizations

Square

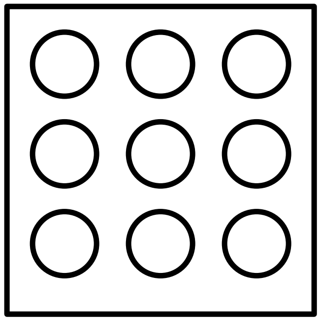

Hexagonal

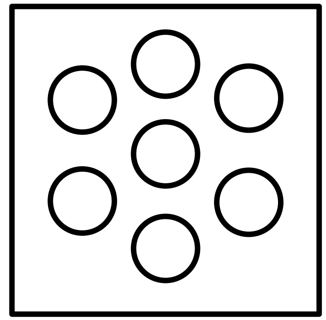

Random
(Poisson process)

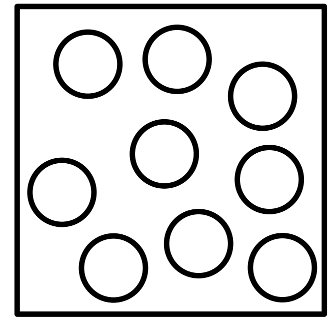

Reality

V_f = 65%

V_f = 22%

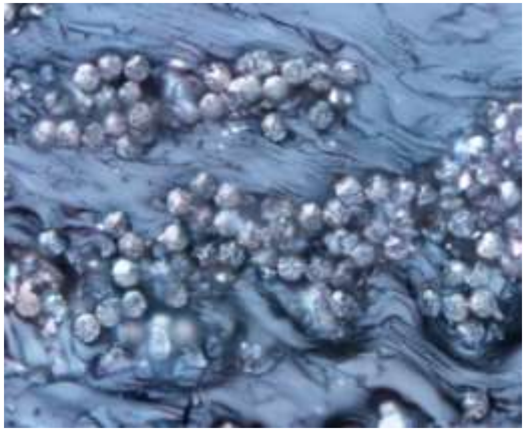

The fibers can be used to calculate the second order intensity function K(r) (Pyrz, 1994)

It measures the average number of fibers within a radial distance from an arbitrary fiber:

$$K(r) = \frac{A}{N^2} \sum_{k=1}^{N} {w_k}^{-1} I_k(r)$$

A	Area considered	N	Total number of fibers
$I_k(r)$	Number of fibers inside a circle of radius r	w_k	Factor introduced to correct edge effects

Reconstruction algorithm (Rintoul and Torquato, 1997) minimizing the following energy:

$$E = \sum_{k} \left(K(r_k) - \tilde{K}(r_k) \right)^2 + \sum_{i} \sum_{j} \left(\left(\frac{100}{d_{ij}} + 10 \right) \delta_{ij} + 100\delta_i \right)$$

FINITE ELEMENT MODELING

Microstructure affects the stress and strain concentrations.

This is very important to model the damage process.

Examples with V_f = 50%

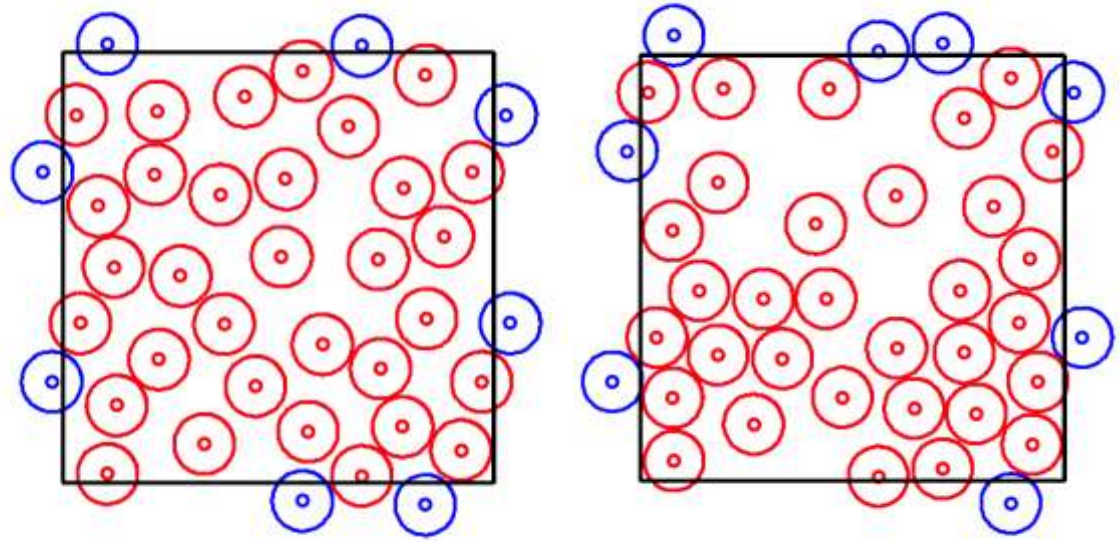

Purely random Reconstructed

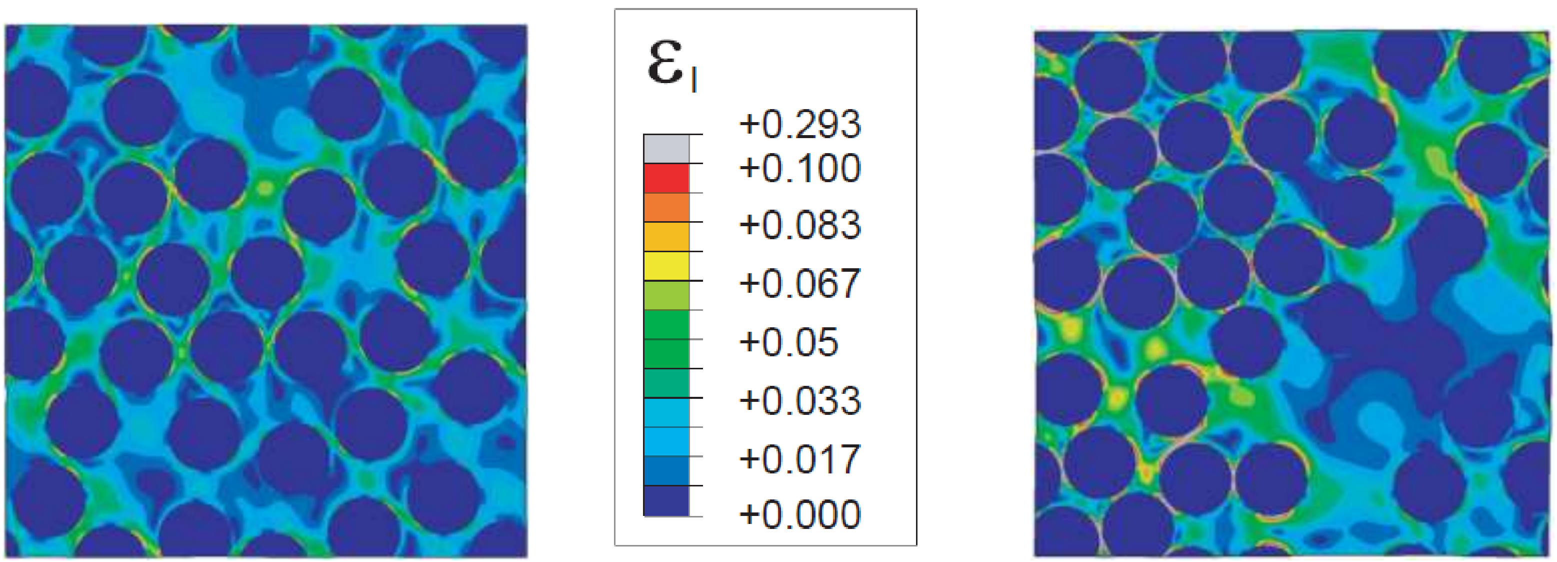

Purely random $\bar{\varepsilon}_y = 1\%$ Reconstructed

The simulation can only capture the initial stiffness.

Cohesive elements introduced to model the damage due to debonding.

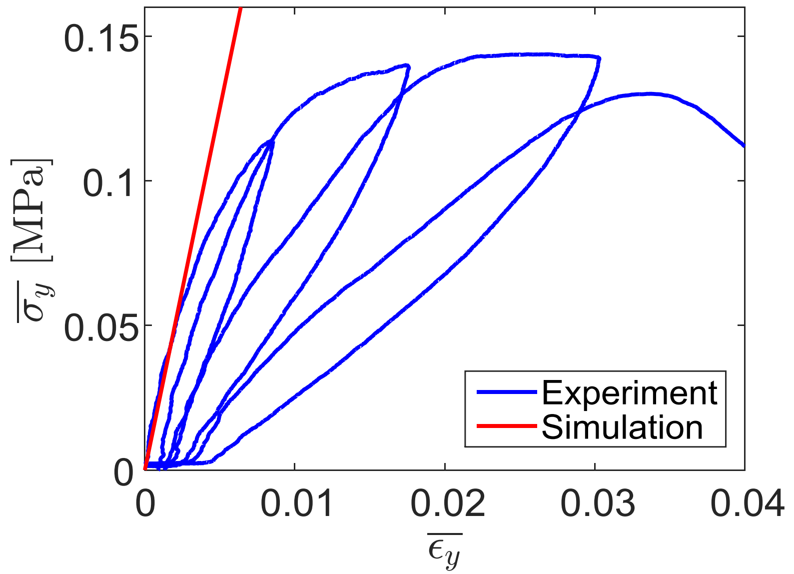

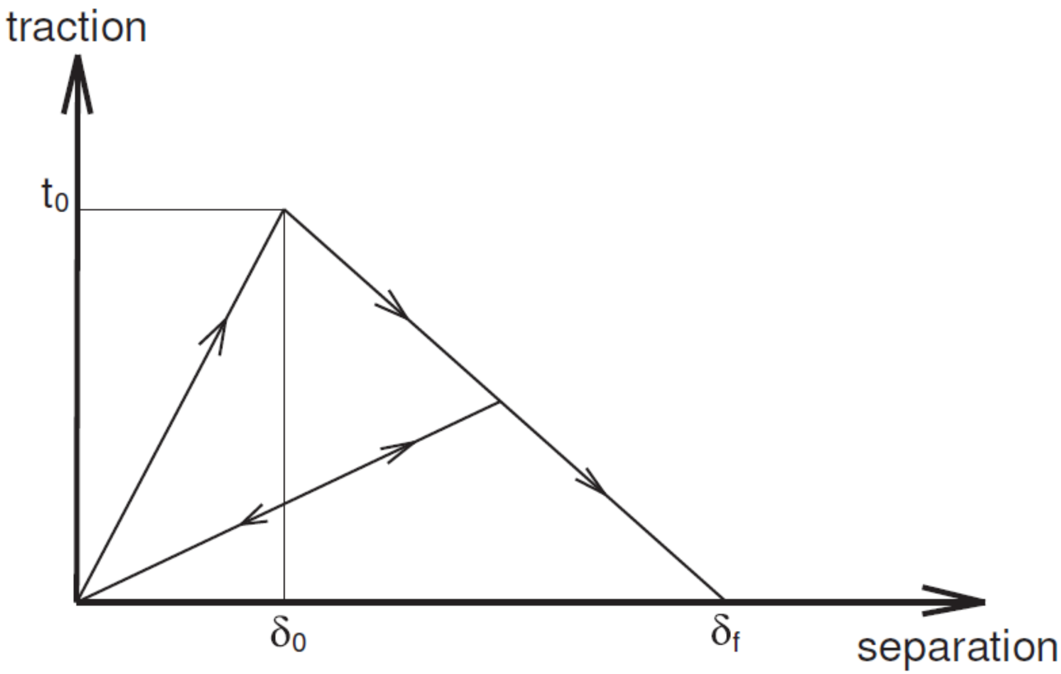

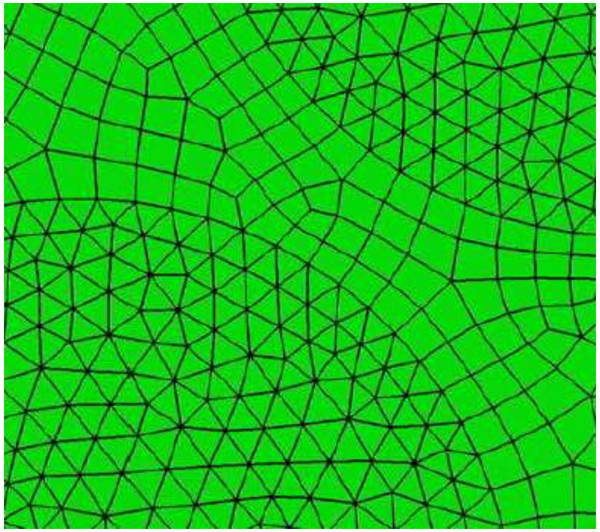

Model with cohesive elements captures:

Nonlinearity.

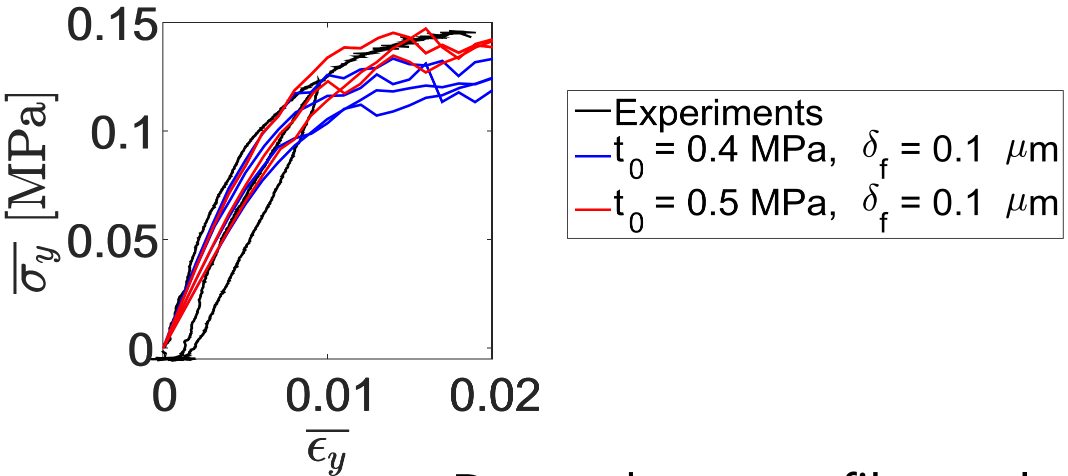

Damage under cyclic loading (no hysteresis)

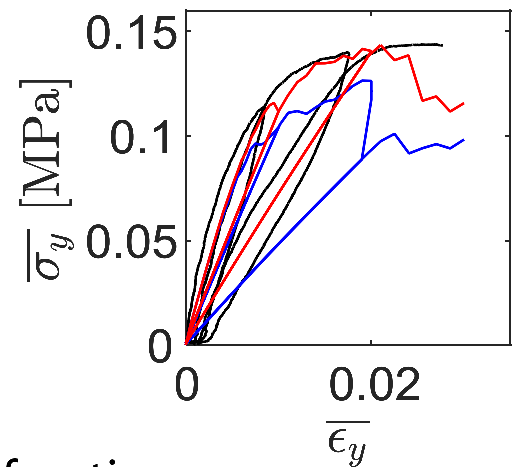

Dependence on fiber volume fraction

V_f = 65%

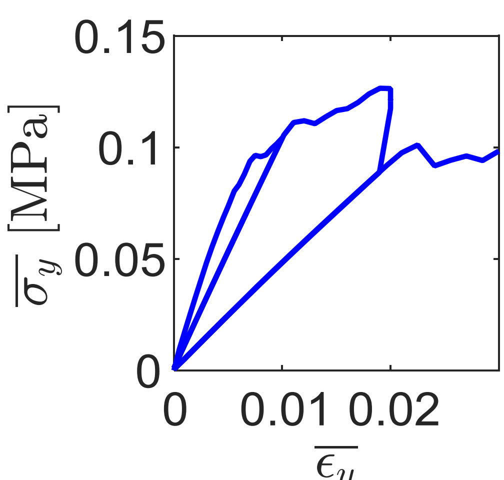

V_f = 22%

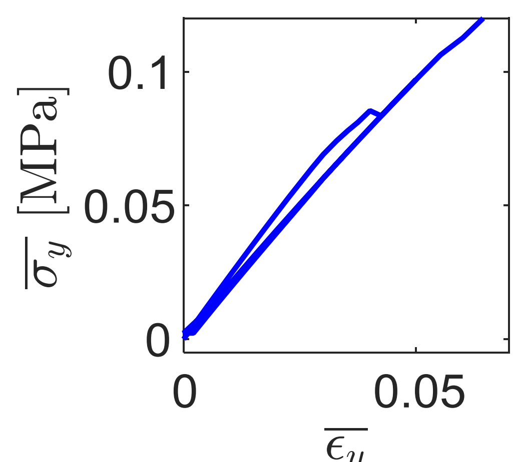

FLJ and Pellegrino, IJSS, 2012

FIBER FAILURE

The model predicts a reduction in fiber strain.

However, this effect is not enough to explain the performance of the material.

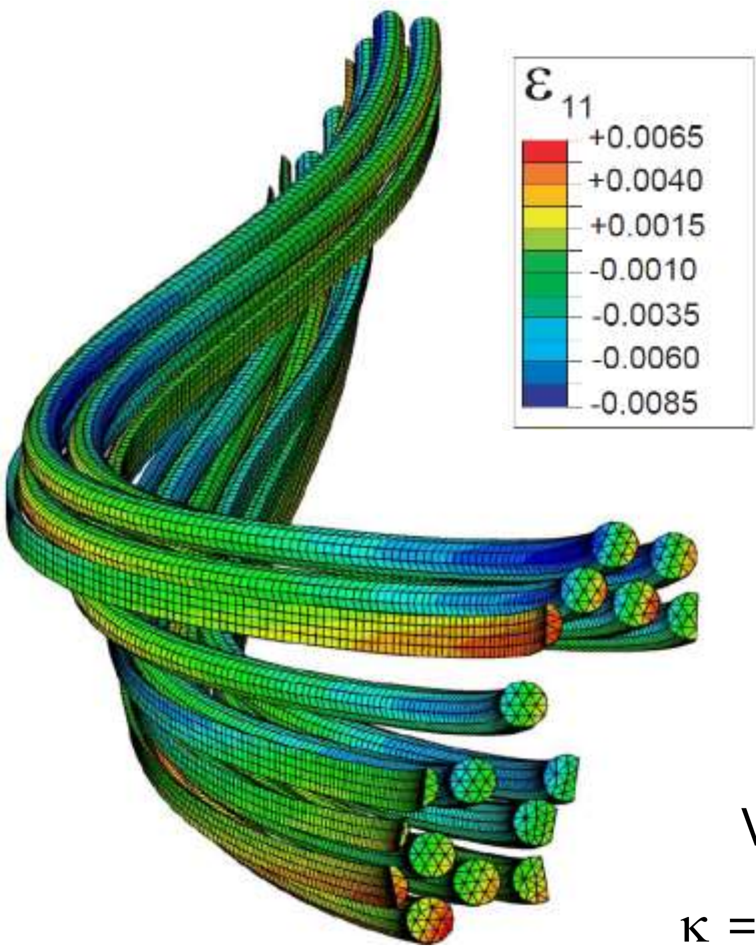

$V_f = 30\%$

$\kappa = 0.35\ mm^{-1}$

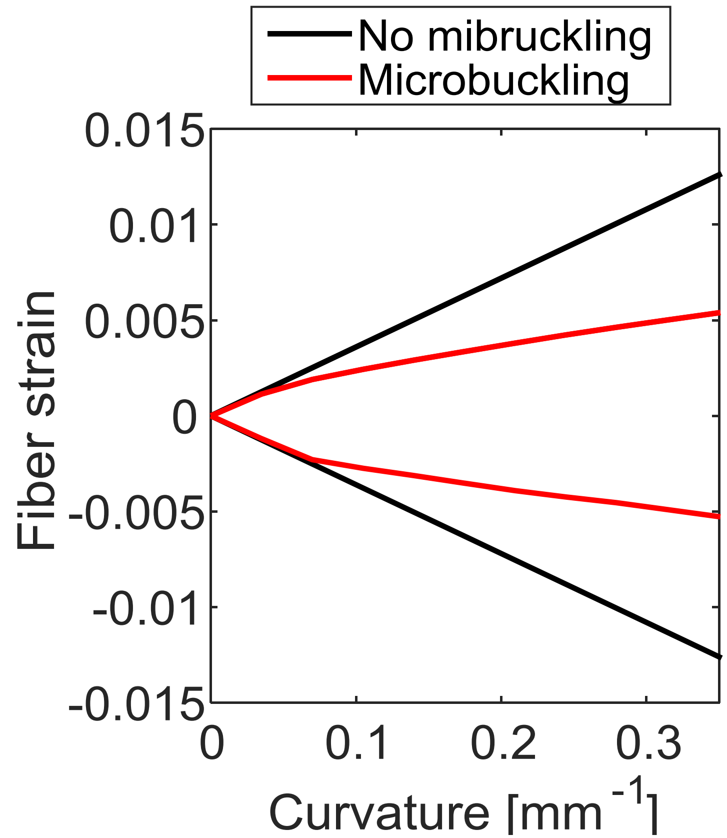

The same happens when single carbon fibers under bending.

This is done with the fiber loop test (Sinclair, 1950):

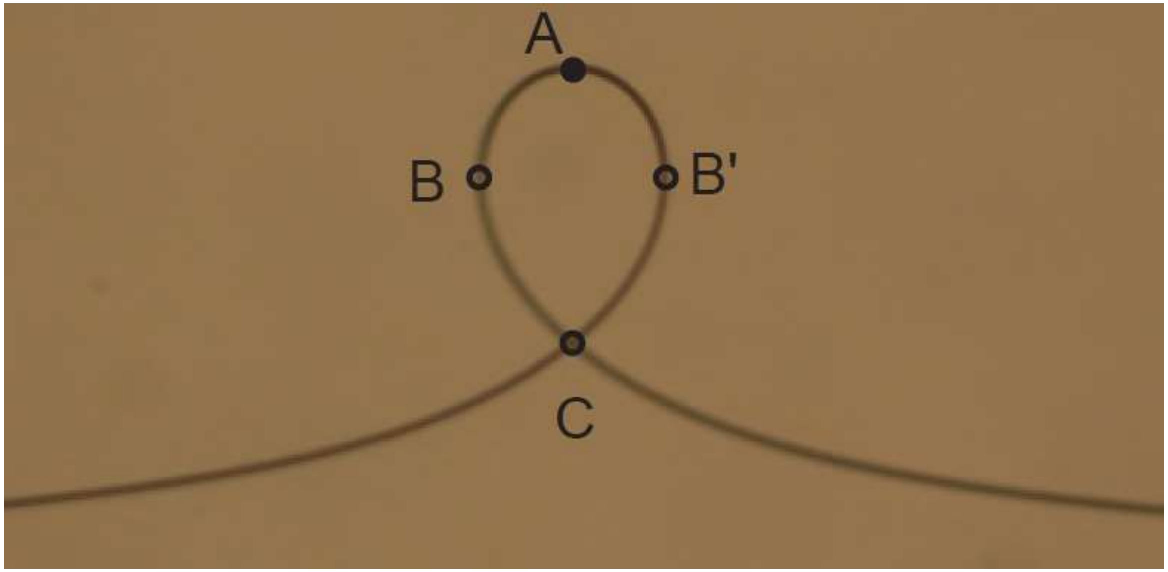

Assuming $\varepsilon = \kappa r$, the maximum strain at A is much higher than the fiber failure strain under uniaxial tension.

FIBER FAILURE

Carbon fiber as a very complicated structure.

Failure is probabilistic in nature, and depends on the presence of flaws.

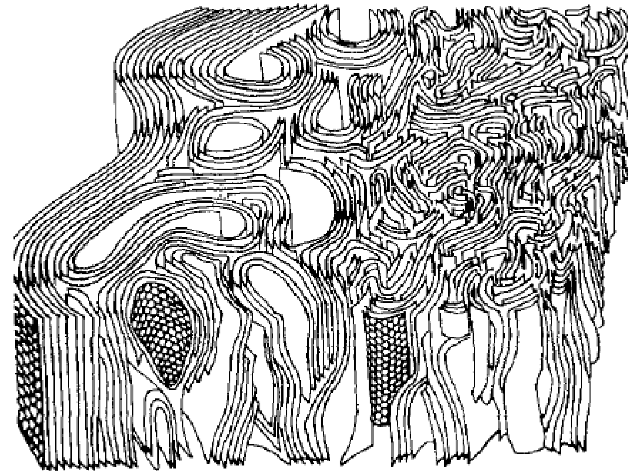

Bennet and Johnson (1978)

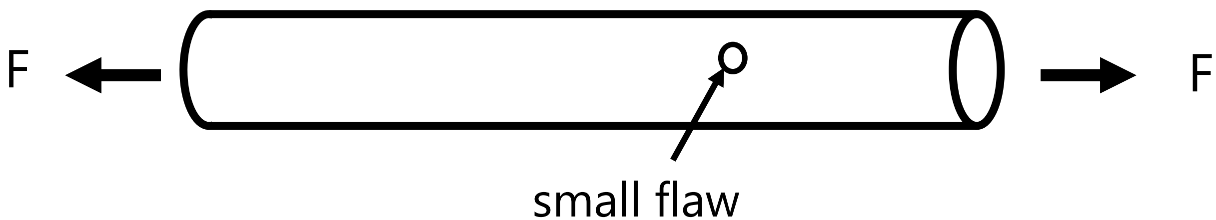

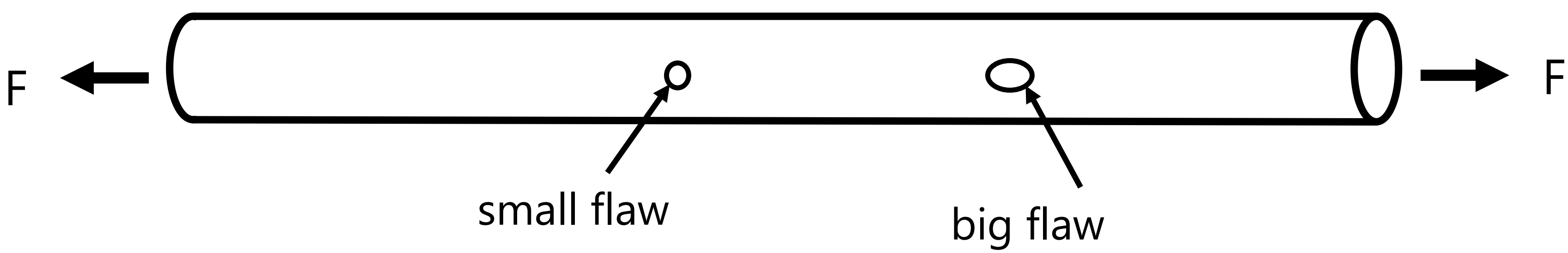

FIBER FAILURE

Under bending the stress is highly localized, so curvature failure is higher than expected.

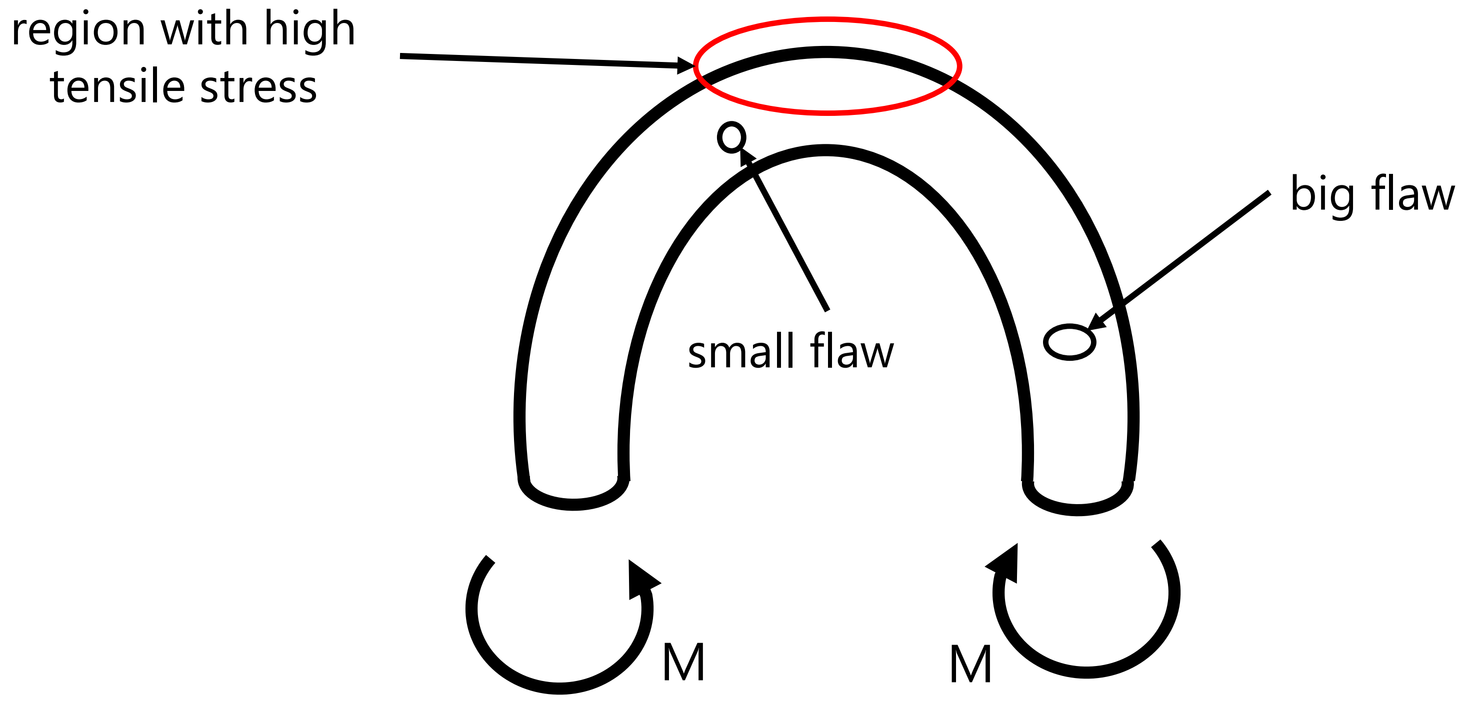

Can we connect tension and bending?

FIBER FAILURE

Brittle failure is modeled with a Weibull distribution:

$$P(\sigma, V) = 1 - \exp\left(-\frac{V}{V_0}\left(\frac{\sigma}{\sigma_0}\right)^m\right)$$

V_0 – volume dependence

σ_0 – normalizing stress

The Weibull modulus *m* describes the variability in strength:

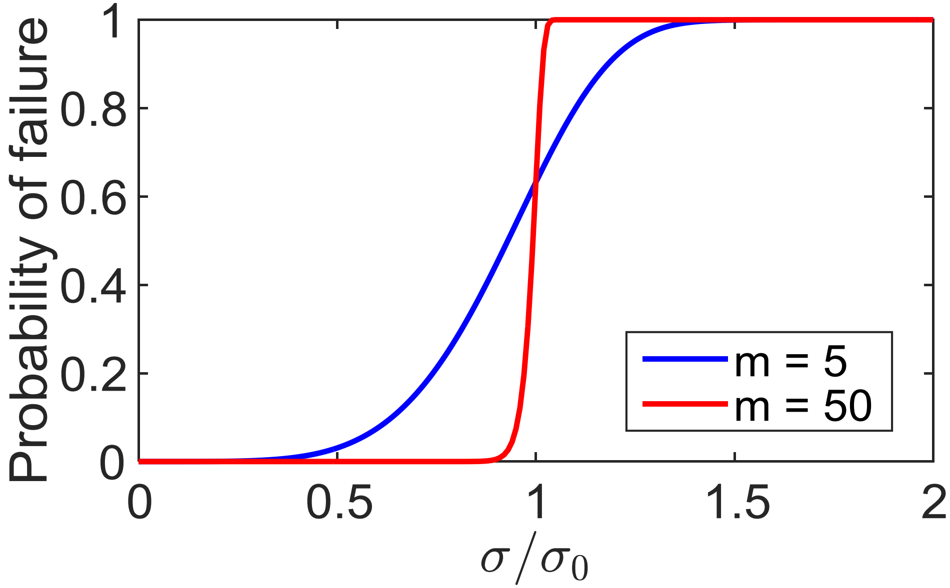

Testing of single fibers provides a description of the failure process.

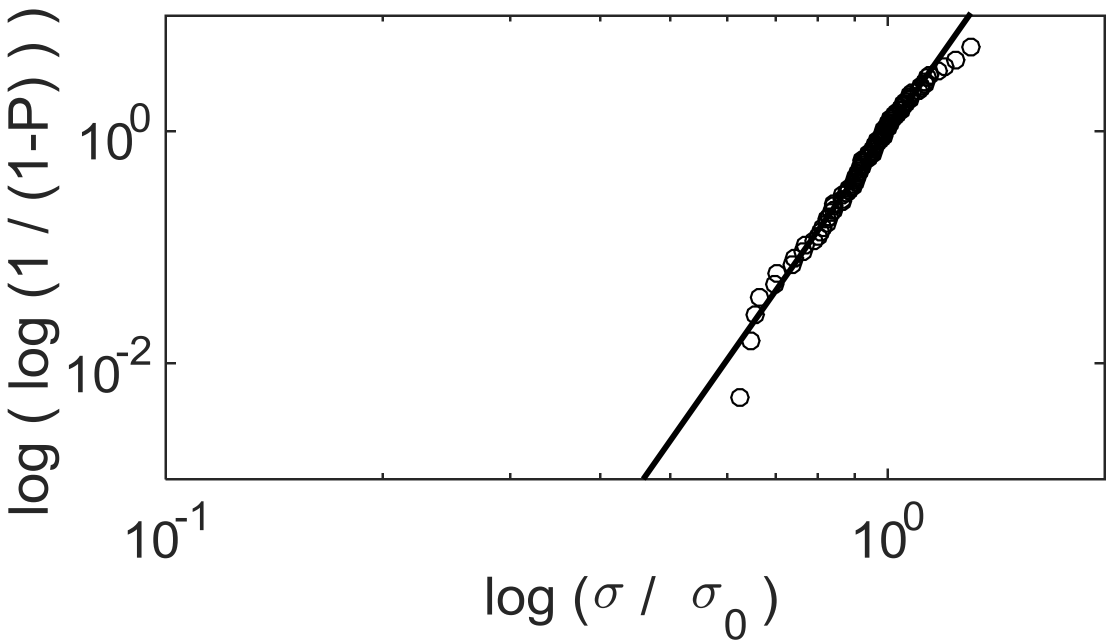

$$P(\sigma, V) = 1 - \exp\left(-\frac{V}{V_0}\left(\frac{\sigma}{\sigma_0}\right)^m\right)$$

σ_0 = 4.68 MPa
m = 10.397
ε_0= 1.89 %

However, this equation is a simplification for pure tension.

For general loading:

$$P = 1 - \exp\left(-\frac{1}{\sigma_0^m V_0}\int_{V_t}\sigma^m dV\right)$$

For pure bending: $\sigma = E_t \kappa \eta$

$$P = 1 - \exp\left(-\frac{1}{\sigma_0^m V_0}\int_0^L \int_{A_t}\left(E_t \kappa(s)\eta\right)^m dA\,ds\right)$$

Loop test can be analyzed using Euler's elastica.

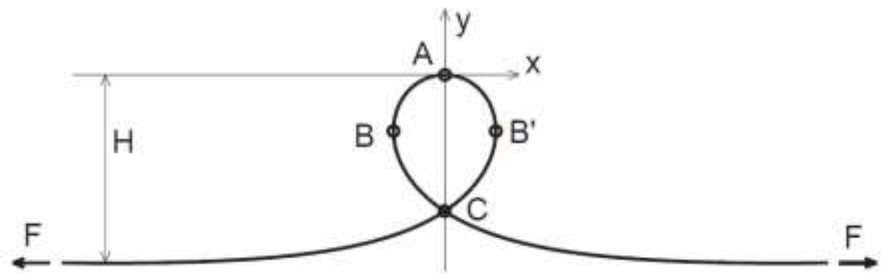

Failure as function of curvature

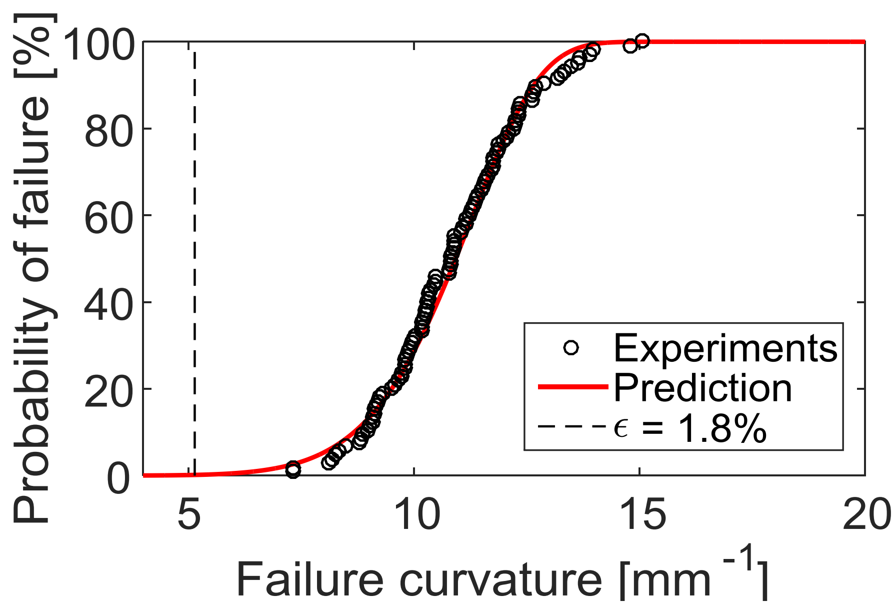

FIBER FAILURE

In the case of fiber microbuckling in the composite:

Wavelength: $$\lambda = \lambda_0(1 - \kappa t)$$ $$\lambda_0 = \left(\frac{9\pi^3 V_f t^2 EI}{8R^2 \log\left(\frac{3t}{b}\right) G} \right)^{\frac{1}{4}}$$

Francis et al., 2007

Amplitude: $$\int_0^1 \sqrt{1 + \left(\frac{a}{\lambda}\pi \cos \pi \hat{x}\right)^2}\, d\hat{x} = \frac{1}{1 - \kappa t}$$

To compare, specimens of 0.5 mm thickness folded to different curvatures. We then calculate the percentage of broken fibers.

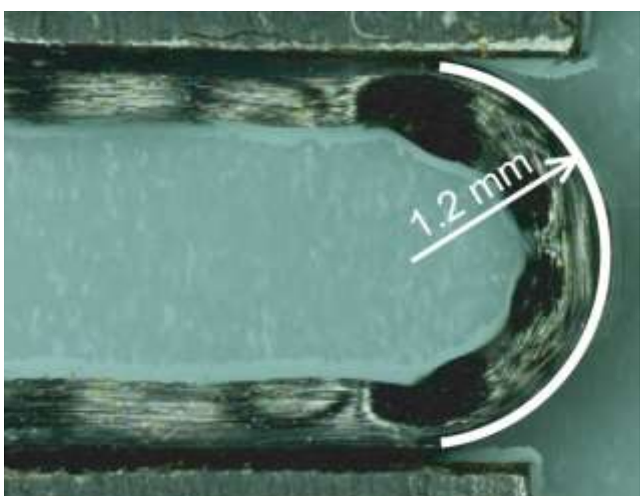

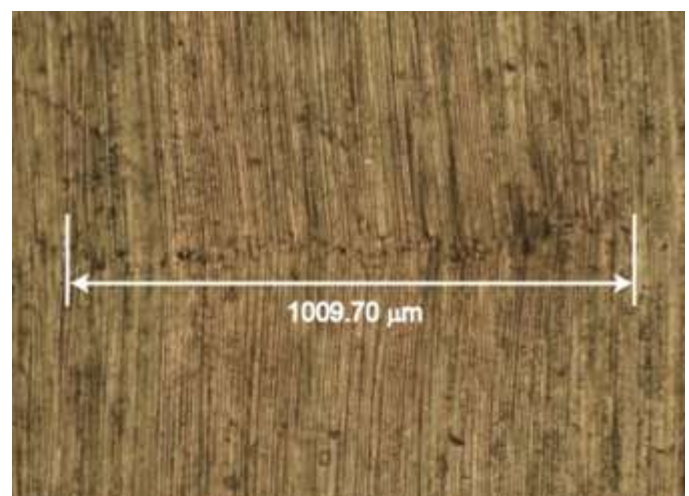

FIBER FAILURE

The model is able to predict the initiation of failure.

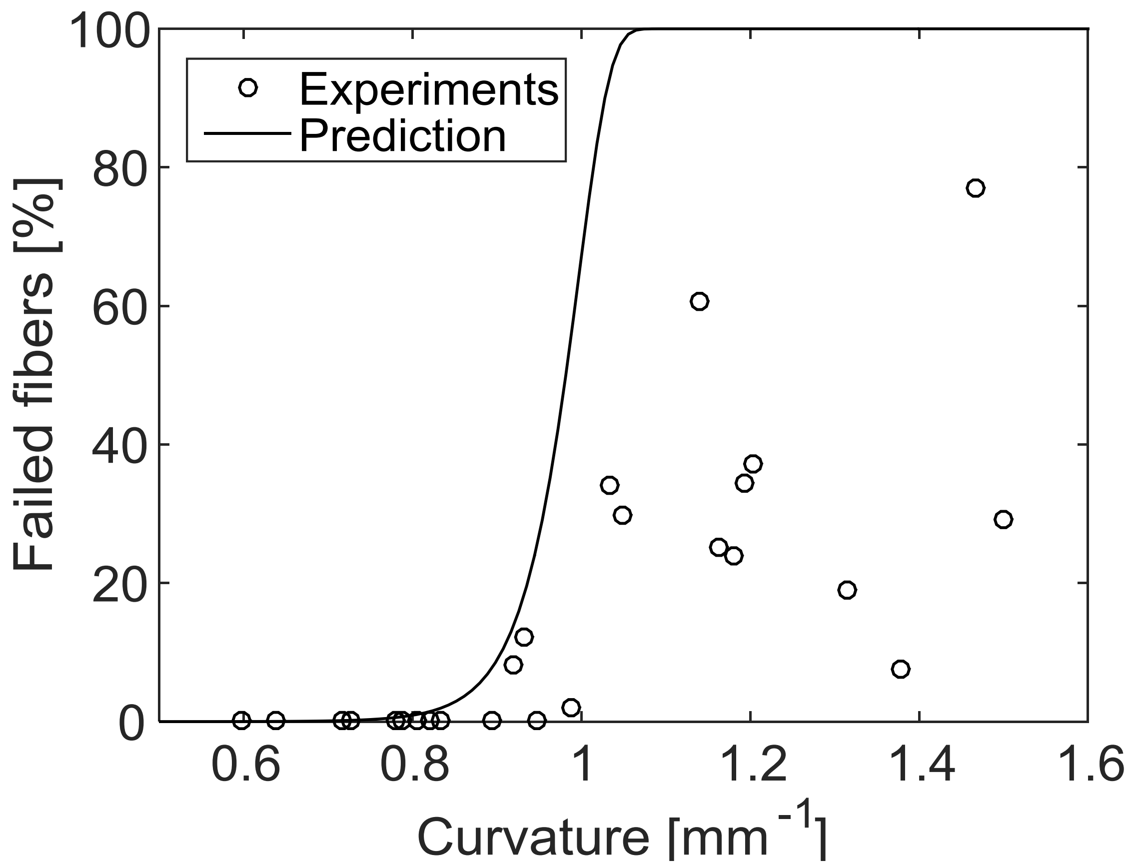

FLJ and Pellegrino, JAM, 2013

HOMOGENIZATION

Numerical simulations useful to understand the mechanics.

The design of structures requires a simple homogenized response.

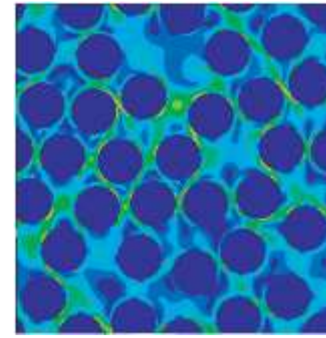

Homogenization not only important in fiber composites:

Magnetorheological elastomers

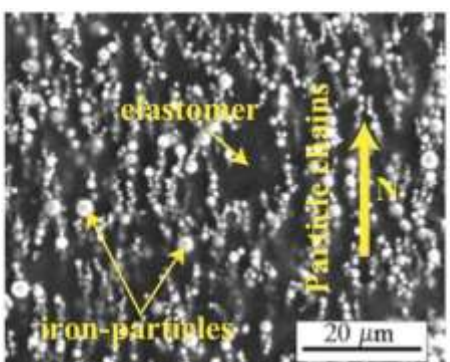

Danas et. al (2012)

Polycrystalline materials

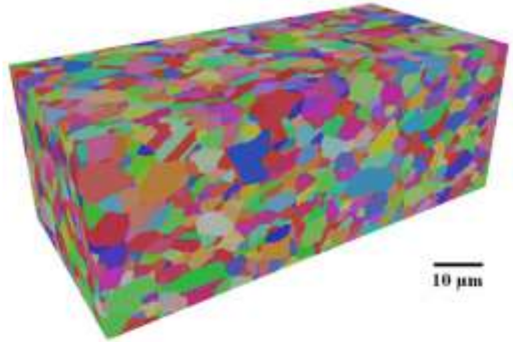

Groeber et. al (2008)

Biological tissue

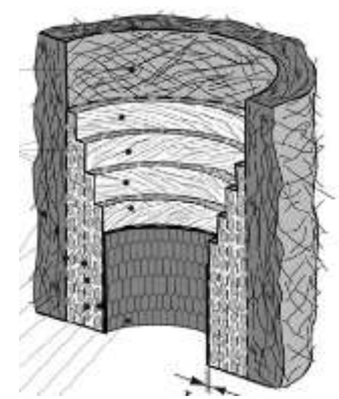

Holzapfel et. al (2001)

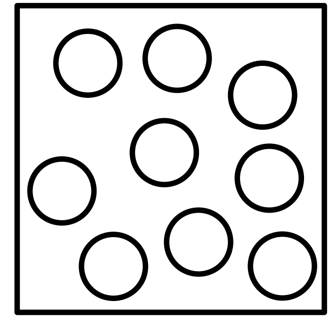

Nonlinear homogenization:

Strain energy of heterogeneous materials:

$$\overline{W}\left(\overline{\mathbf{F}}\right) = \min_{\mathbf{F}\in K\left(\overline{\mathbf{F}}\right)} \frac{1}{V}\int_V W\left(\mathbf{F},\mathbf{X}\right) d\mathbf{X}$$

where: $$\overline{\mathbf{F}} = \frac{1}{V}\int_V \mathbf{F}\left(\mathbf{X}\right) d\mathbf{X}$$

Homogenization techniques aim to provide a prediction:

$$\tilde{W}\left(\overline{\mathbf{F}}\right) \approx \overline{W}\left(\overline{\mathbf{F}}\right)$$

Normally expressed as a function of the deformation invariants:

$$\tilde{W}\left(\overline{I}_1, \overline{I}_2, \overline{I}_3, \overline{I}_4, \overline{I}_5\right) \approx \overline{W}\left(\overline{\mathbf{F}}\right)$$

Several predictions exist, with explicit solutions for Neo-Hookean composites.

Iterative homogenization:

$$\tilde{W}_{IH} = \frac{\tilde{\mu}_{IH}}{2}\left(\overline{I}_1 - 3\right) + \frac{\tilde{\mu}_n - \tilde{\mu}_{IH}}{2}\left(\frac{2}{\sqrt{\overline{I}_4}} - 3\right) + \frac{\tilde{\mu}_n - \tilde{\mu}_{HS}}{2}\overline{I}_4$$

Sequentially coated composites:

$$\tilde{W}_{SCC} = \tilde{\mu}_{HS}\left(\overline{I}_1 - 3\right) + \frac{\tilde{\mu}_n - \tilde{\mu}_{HS}}{2}\frac{\left(\sqrt{\overline{I}_4} + 2\right)\left(\sqrt{\overline{I}_4} - 1\right)^2}{\sqrt{\overline{I}_4}}$$

$$\tilde{\mu}_n = \left(1 - V_f\right)\mu_m + V_f\mu_f$$

$$\tilde{\mu}_{HS} = \frac{\left(1 - V_f\right)\mu_m + \left(1 + V_f\right)\mu_f}{\left(1 + V_f\right)\mu_m + \left(1 - V_f\right)\mu_f}\mu_m$$

$$\tilde{\mu}_{IH} = \left(1 - V_f\right)^2\left(1 + \frac{2\left(2 - V_f\right)V_f}{\left(1 - V_f\right)^2}\frac{\mu_f}{\mu_m} + \frac{\mu_f^2}{\mu_m^2}\right)\frac{\mu_m}{2}$$
$$- \left(1 - V_f\right)^2\sqrt{\frac{2}{\left(1 - V_f\right)^2}\frac{\mu_f}{\mu_m} + \left(1 + \frac{2\left(2 - V_f\right)V_f}{\left(1 - V_f\right)^2}\frac{\mu_f}{\mu_m} + \frac{\mu_f^2}{\mu_m^2}\right)\frac{\mu_f - mu_m}{2}}$$

deBotton (2005)
Lopez-Pamies and Ponte Castañeda (2006)
deBotton et al. (2006)
Agoras et al. (2009)
Lopez-Pamies and Idiart (2010)

HOMOGENIZATION

Numerical homogenization for nonlinear general 3D loading.

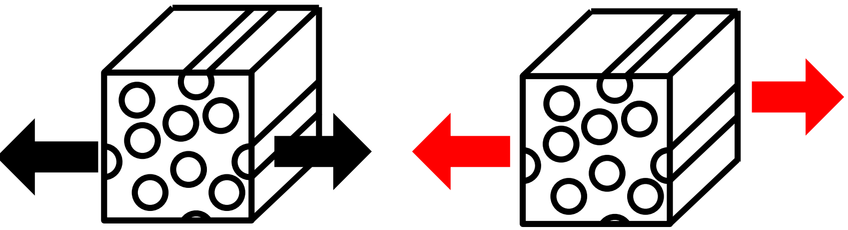

In-plane deformation

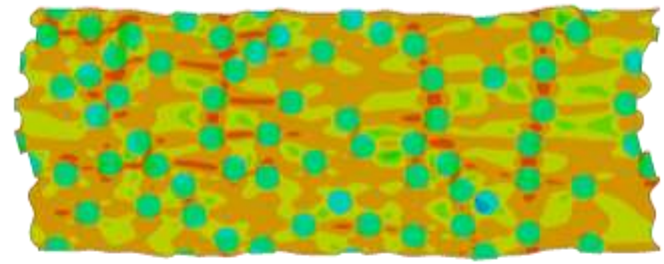

Out-of-plane deformation

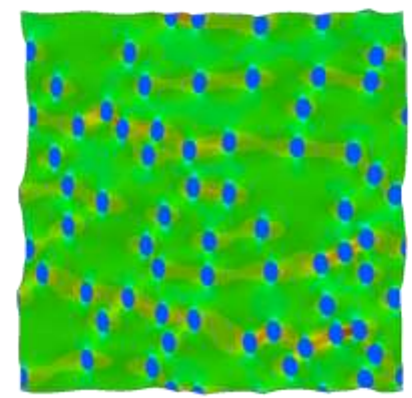

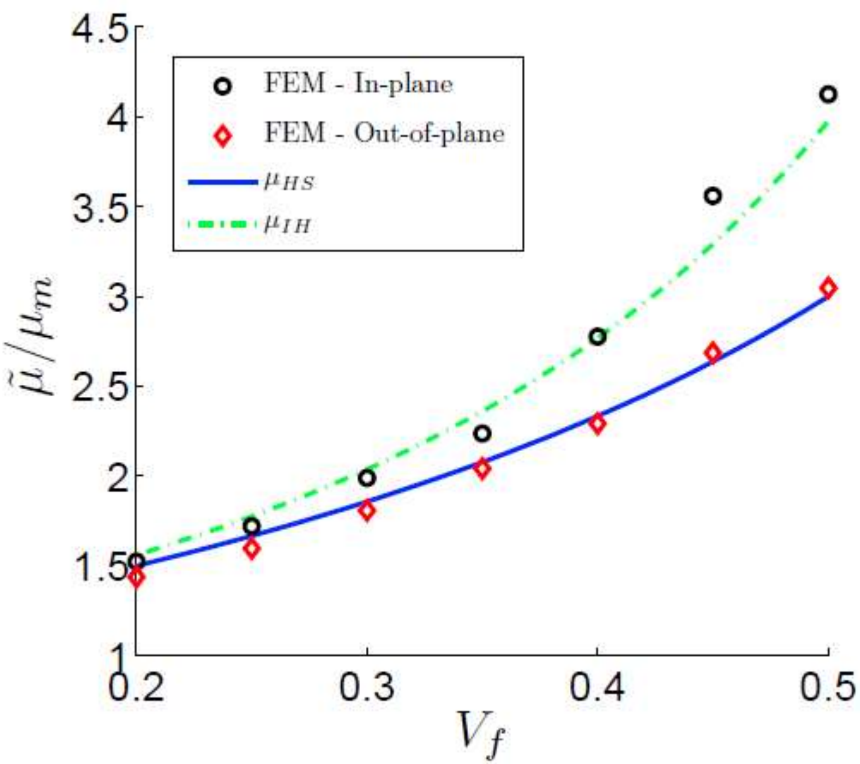

Combined model for all loadings

$$\tilde{W} = \frac{\tilde{\mu}_{IH}}{2}\left(\overline{I}_1 - 3\right) + \frac{\tilde{\mu}_n - \tilde{\mu}_{IH}}{2}\left(\frac{2}{\sqrt{\overline{I}_4}} - 3\right)$$

$$+ \frac{\tilde{\mu}_n - \tilde{\mu}_{HS}}{2}\overline{I}_4 - \frac{\tilde{\mu}_{IH} - \tilde{\mu}_{HS}}{2}\frac{\overline{I}_5}{\overline{I}_4}$$

FLJ, Composites B, 2014

PATTERN FORMATION IN SOFT SOLIDS

Collaboration with:

Prof. Pedro Reis (MIT)

Prof. Jorn Dunkel (MIT, Mathematics)

Dr. Romain Lagrange (MIT, Mathematics)

Dr. Norbert Stoop (MIT, Mathematics)

Dr. Denis Terwagne (Universite Libre de Bruxelles)

MOTIVATION AND BACKGROUND

A thin film on a soft elastic foundation wrinkles under compression:

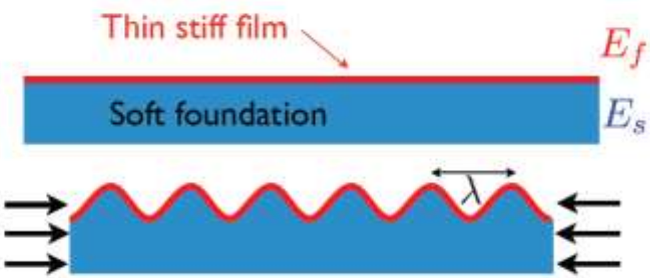

$$\lambda = \left(\frac{2\pi}{3^{1/3}}\right) h \left(\frac{E_f}{E_s}\right)^{1/3}$$

$$\sigma_0^C = \frac{3^{2/3}}{4} {E_f}^{1/3} {E_s}^{2/3}$$

Allen (1969)

Biaxial compression:

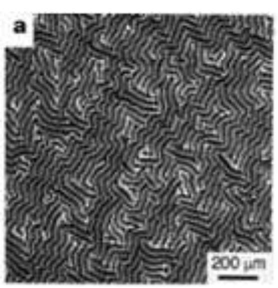

Bowden et al. (1998)

Energy minimization:

Observed experimentally:

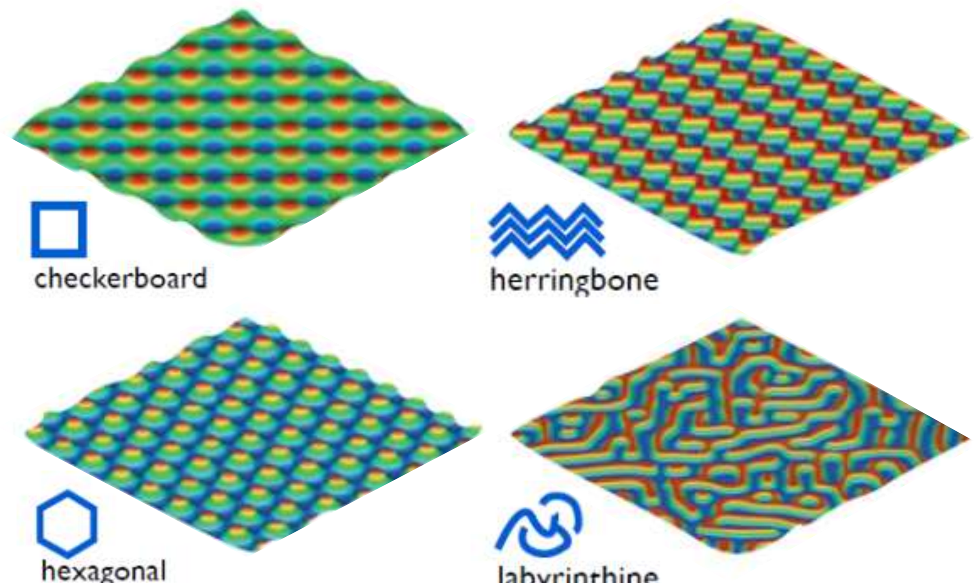

Audoly and Boudaoud (2008), Cai et al. (2011)

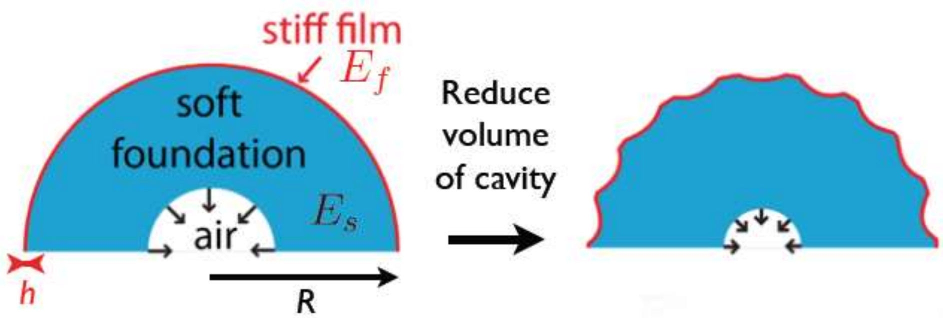

$E_f = 2500kPa$
$E_s = 350kPa$
$\lambda \approx 3mm$
$D = 40mm$
$h = 480\mu m$

Drag reduction:

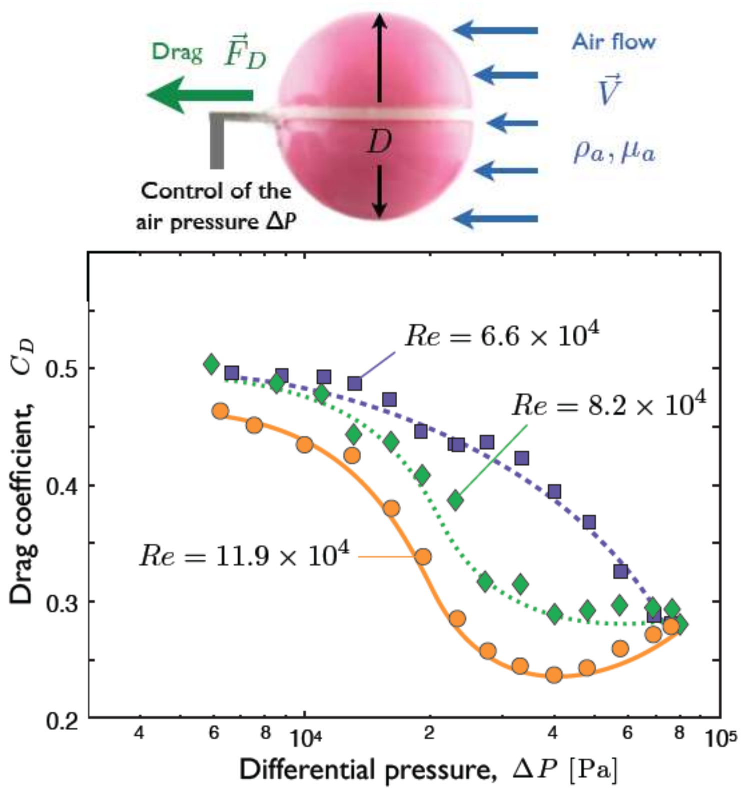

Effect of curvature on wrinkling:

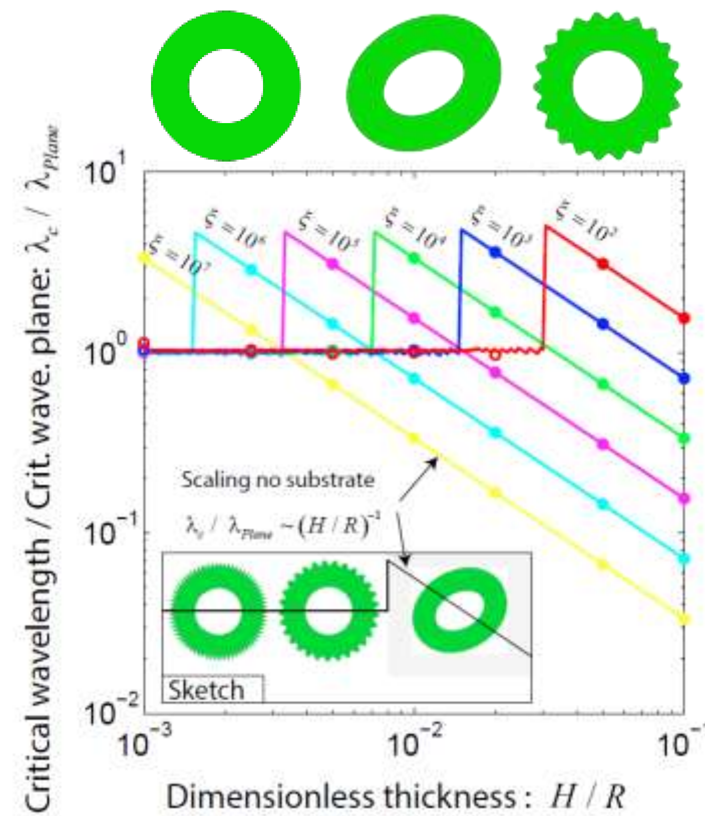

Terwagne et al. (2014)

Lagrange, FLJ, Terwagne, Brojan, Reis (JMPS, in review)

MODELING WRINKLING ON CURVED SURFACES

Collaboration with Norbert Stoop and Jorn Dunkel (MIT Math)

The energy minimization in the film can be rewritten as a modified Swift-Hohenberg equation:

$$\partial_t u \;=\; \gamma_0 \Delta u - \gamma_2 \Delta^2 u - au - bu^2 - cu^3 + \;(\Gamma_1 + \Gamma_2 u)\cdot\left[(\nabla u)^2 + 2u\Delta u\right]$$

stretching

bending

local film and substrate

higher order stretching

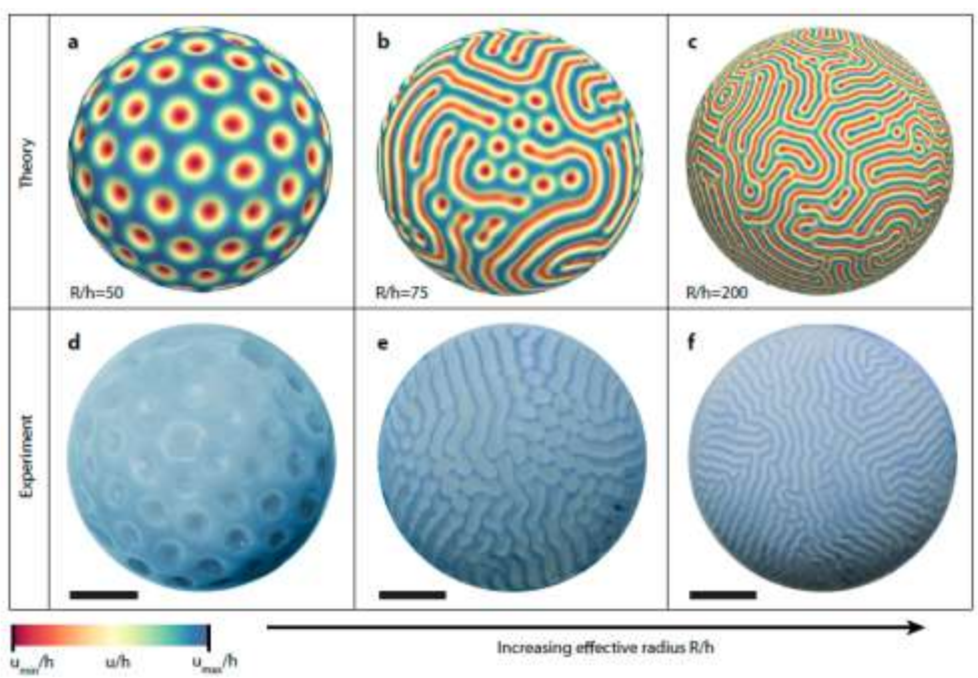

Stoop et. al (2015)

CRYSTALLOGRAPHY IN 3D

Goal:

Treat dimples as lattice elements.

Study the effect of curvature on crystal structures.

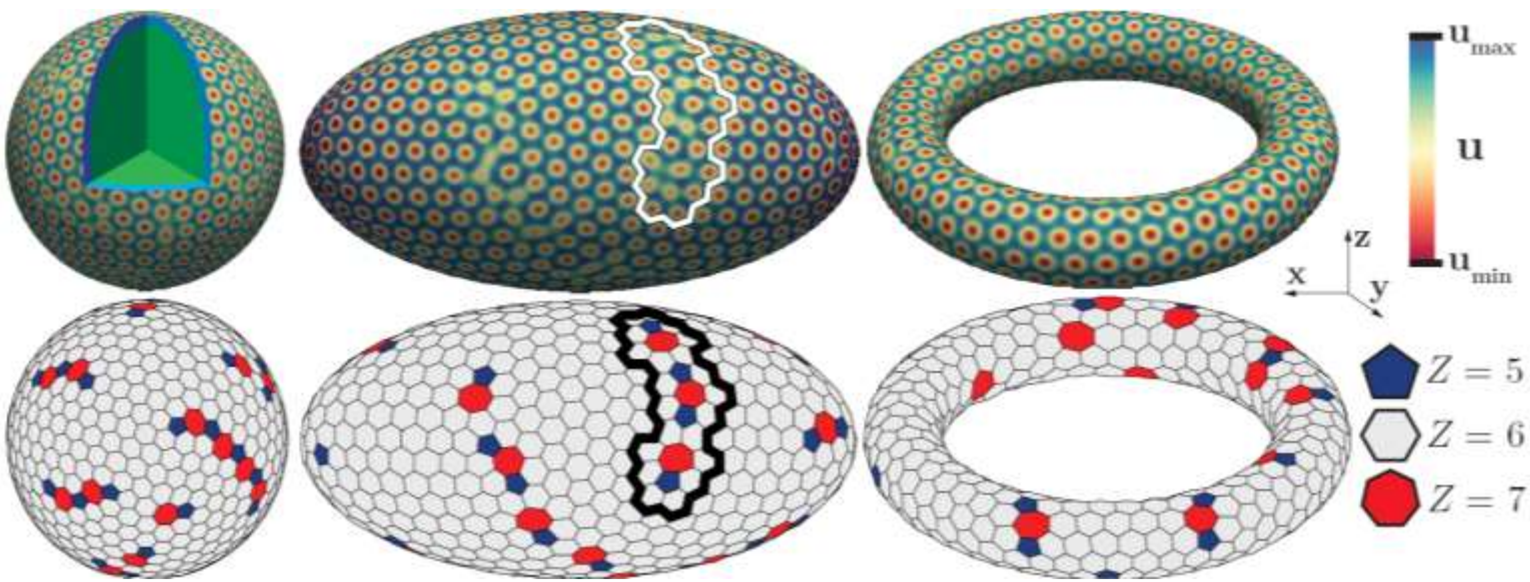

Sphere
$R = 70\ \lambda$

Ellipsoid
$R_x = 2\ R_y = 2\ R_z = 100\ \lambda$

Torus
$R = 5\ r = 80\ \lambda$

Crystallography shown to be independent of the physical potential (Bowick et al., 2002; Bausch et al., 2003)

CRYSTALLOGRAPHY IN 3D

Planar crystals tend to arrange in regular lattices.

A hexagonal lattice is space-filling and usually minimizes energy.

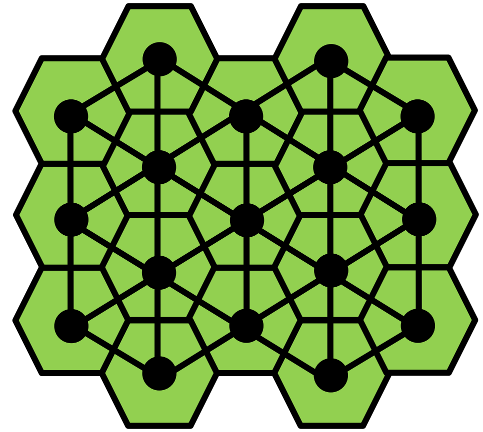

This is not true in 2D crystals in 3D curved surfaces, where defects are necessary.

Some examples:

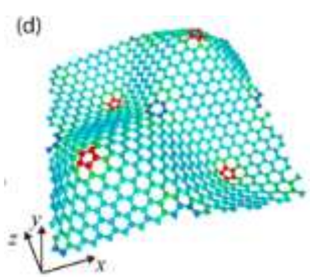

Graphene
(Zhang et al., 2014)

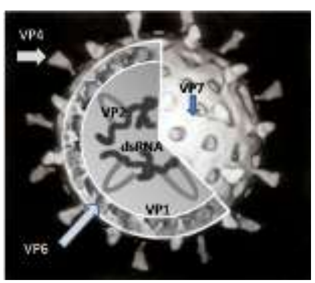

Rotavirus

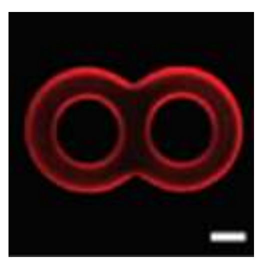

Microcapsules
(Chen et al., 2015)

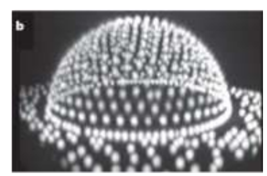

Colloids
(Irvine at al., 2010)

Football

Geodesic dome

CRYSTALLOGRAPHY IN 3D

First, there is a topological need:

Topological charge:

$$s_i = 6 - Z$$

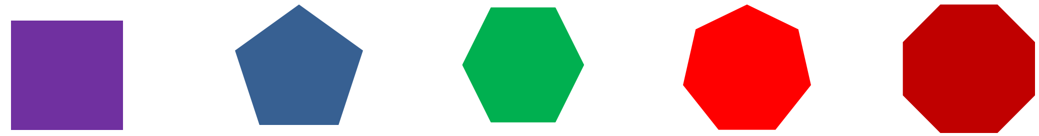

s = 2 s = 1 s = 0 s = -1 s = -2

Euler's rule:

$$\chi = E - V - F$$

Total charge:

$$Q = \sum_i s_i = 6\chi$$

Sphere: $\chi = 2 \ \rightarrow Q = 12$

Torus: $\chi = 0 \ \rightarrow Q = 0$

In a sphere that usually means 12 pentagons:

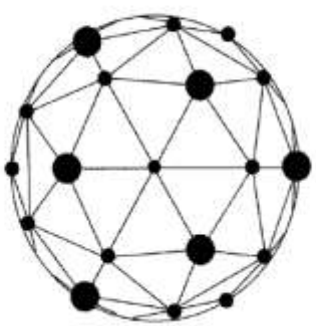

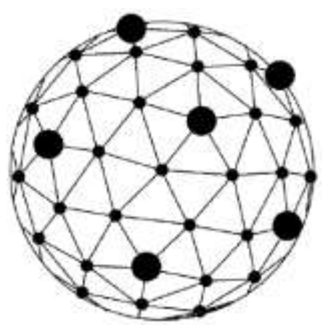

Dodgson (1996)

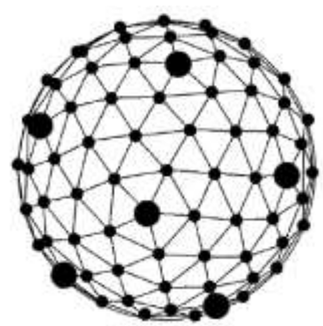

CRYSTALLOGRAPHY IN 3D

Second, defects reduce energy required to conform to surface:

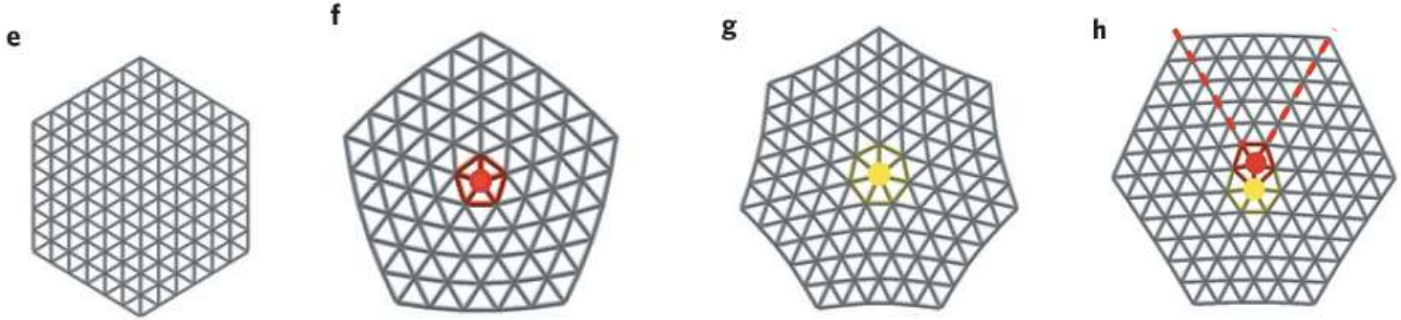

Neutral	Five defect: Positive	Seven defect: Negative	Dislocation: Screens strain

As size increases, more defects appear:

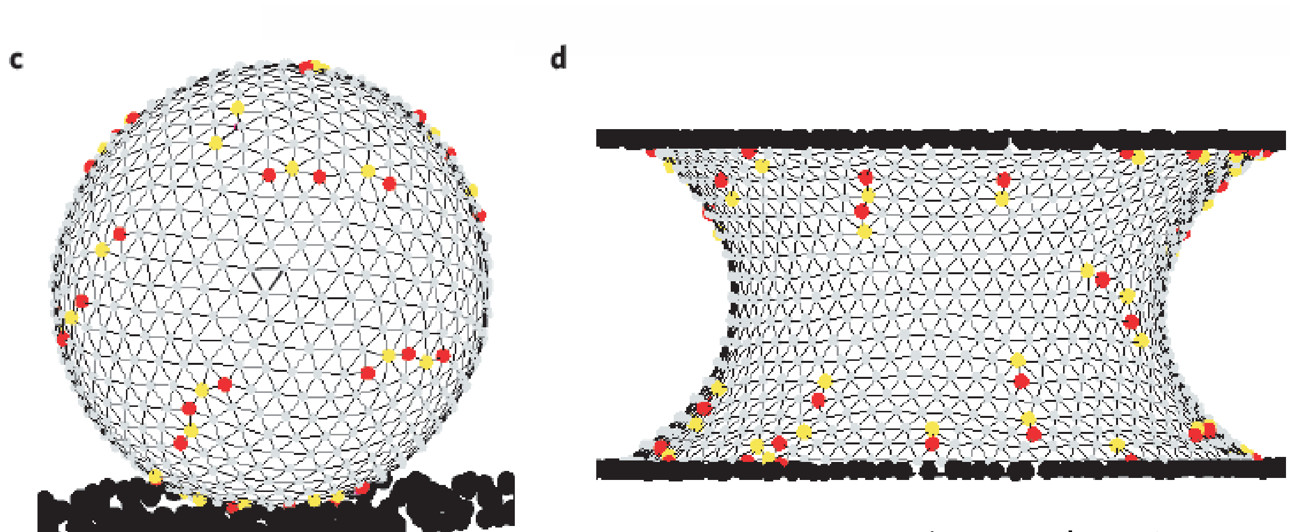

Irvine et al, 2012

EFFECT OF SYSTEM SIZE

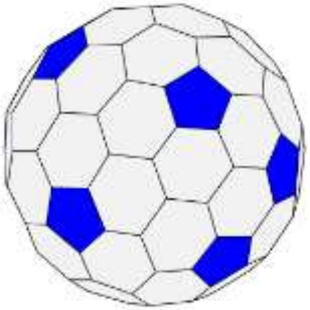

R / λ = 20

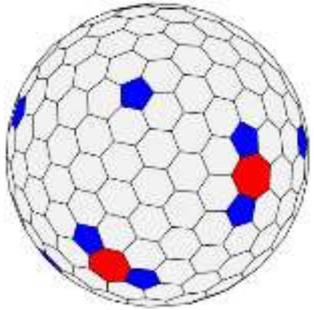

R / λ = 40

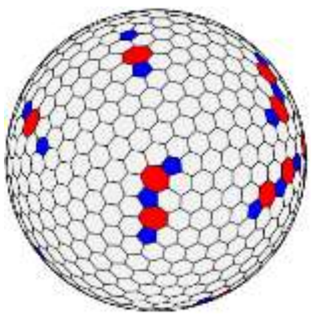

R / λ = 50

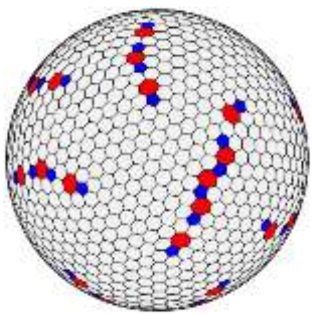

R / λ = 100

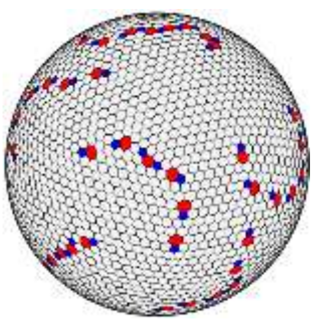

R / λ = 150

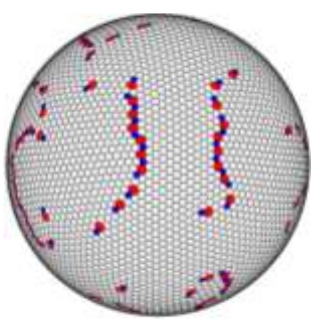

R / λ = 200

Similar scaling for all geometries

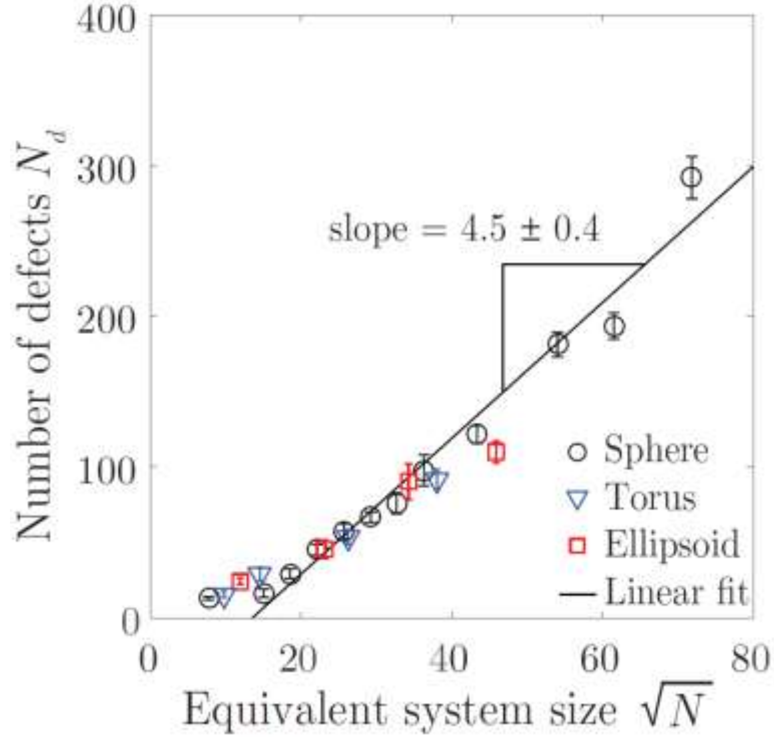

Agreement with results for colloids:

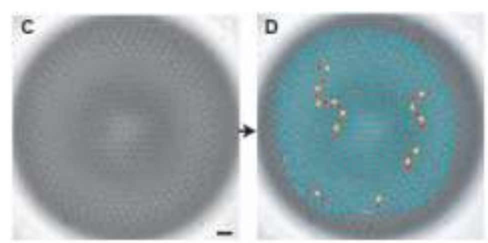

Bausch et al. (2003)

EFFECT OF CURVATURE

Relationship between defects and curvature:

$$\left.\begin{array}{ll}\text{Gauss-Bonnet:} & \int K\,dA = 2\pi\chi \\[2em] \text{Euler:} & \Sigma_i s_i = 6\chi\end{array}\right\} \int K\,dA = \frac{\pi}{3}\Sigma_i s_i$$

If we consider larger caps of each solid:

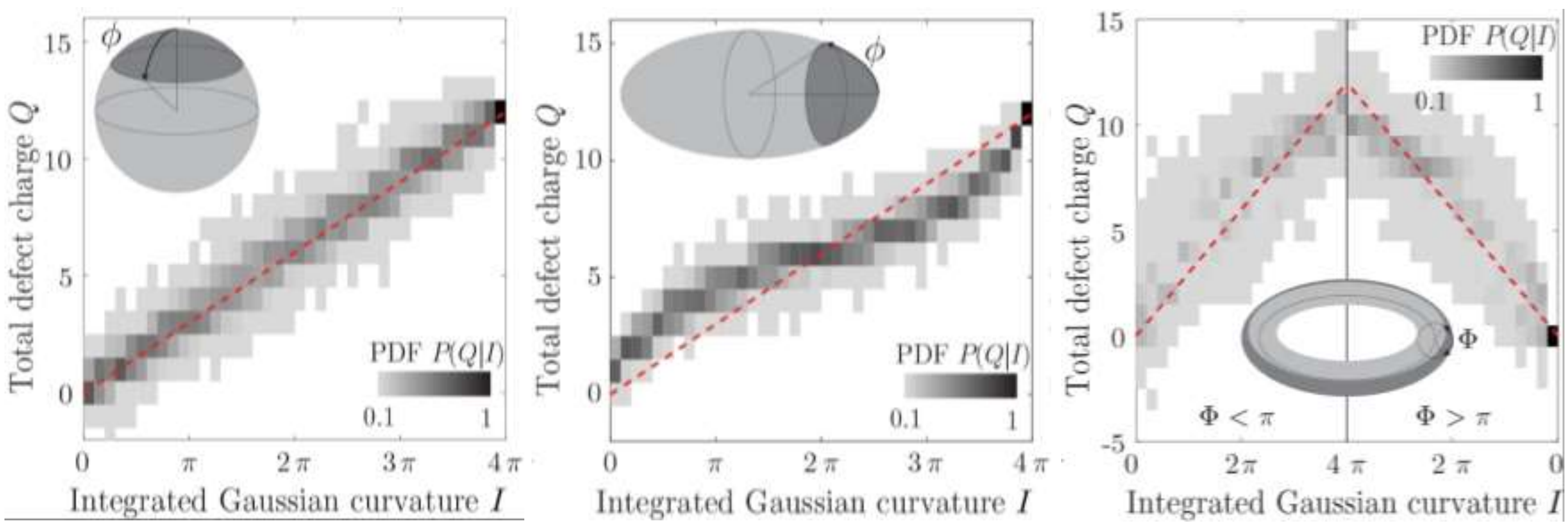

DEFECTS IN ELLIPSOID

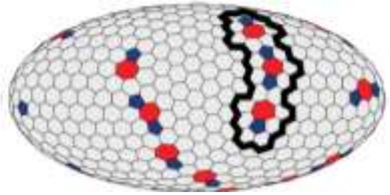

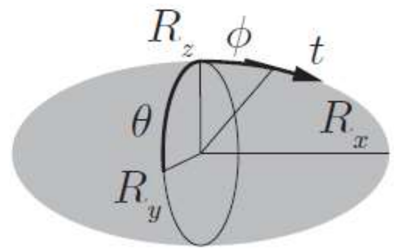

Chains:

- Position of centroids
- α: Angle between end-to-end vector and tangent **t**

Single defects

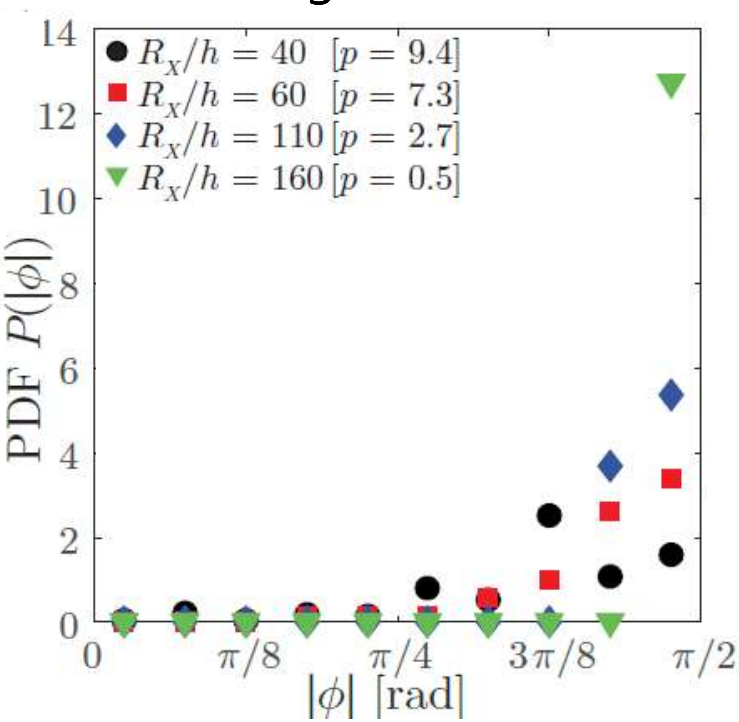

Defect chains

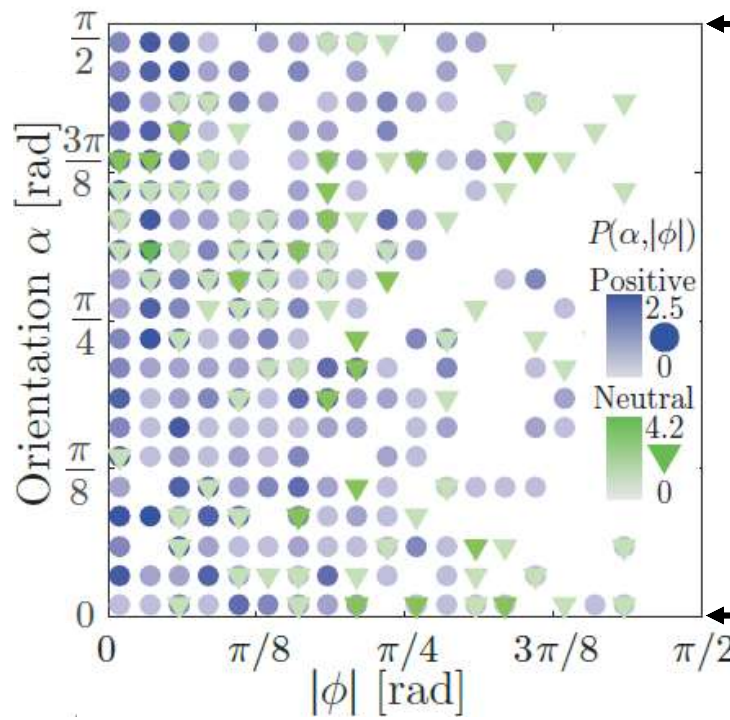

Parallel to equator

Along poles

DEFECTS IN TORUS

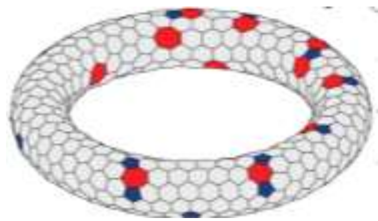

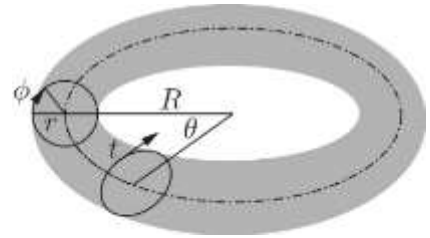

Chains:

- Position of centroids
- α: Angle between end-to-end vector and tangent **t**

Single defects

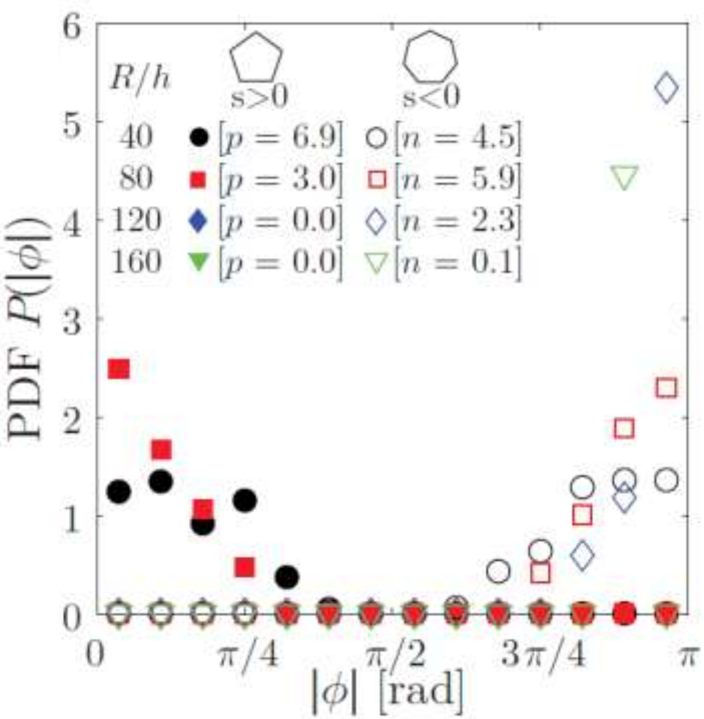

Defect chains

Along R (or θ)

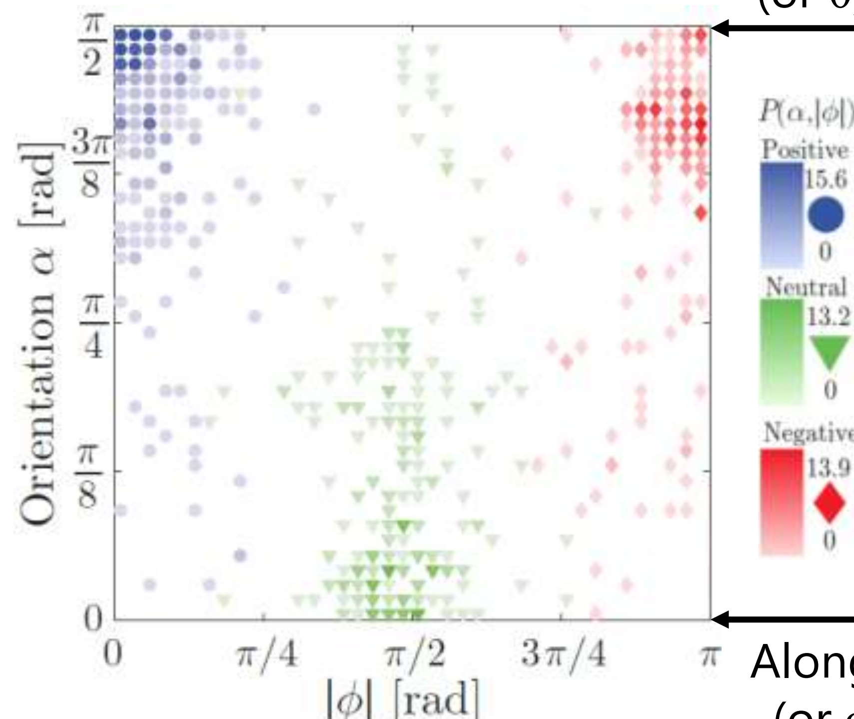

Along r (or ϕ)

GLOBAL STRUCTURE IN TORUS

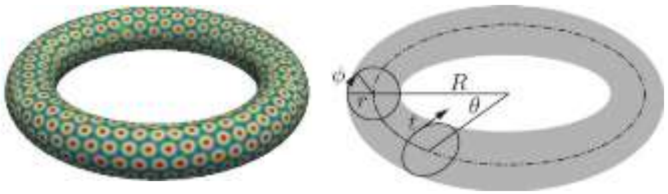

Location and structure of defects

Positive: 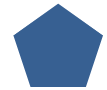 Negative: 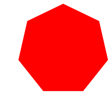

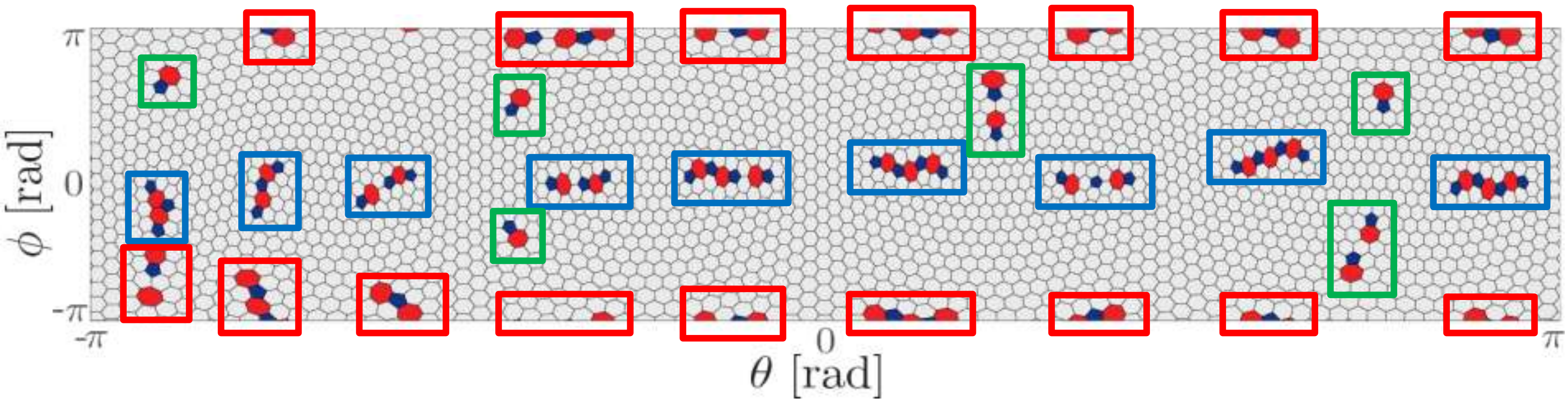

Positive chains: Approximately eight, equidistant, along outer side.

Negative chains: Same number, inner side.

Neutral chains: Between pairs of charged chains, in regions with zero gaussian curvature, perpendicular aligment.

Arrangement of chains can be interpreted as charged particles in an electric field. (Bowick et al., 2004)

GLOBAL STRUCTURE IN TORUS

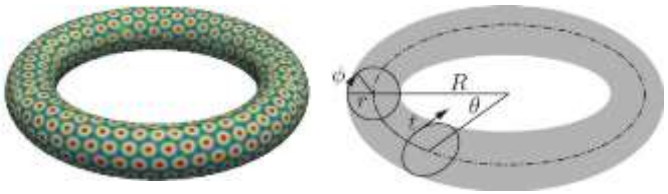

PDF of distance between centroid of chains shows alignment.

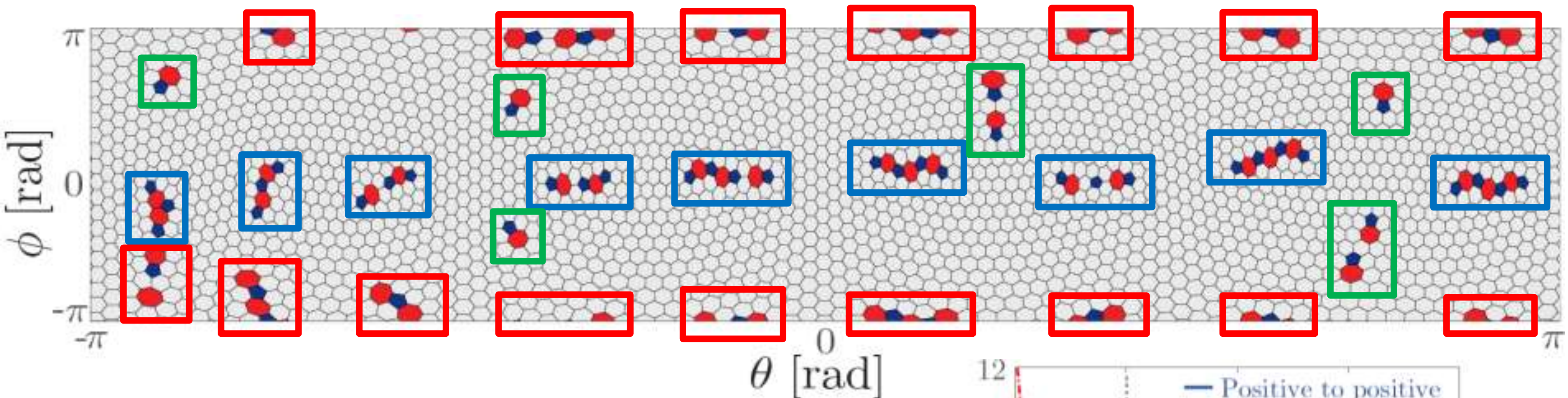

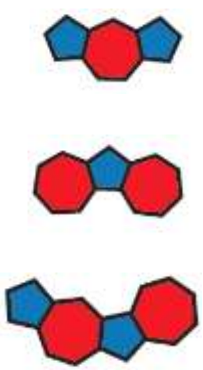

Positive to positive: Δθ = π/4

Negative to positive: Δθ = 0.

Neutral to positive: Δθ = π/8.

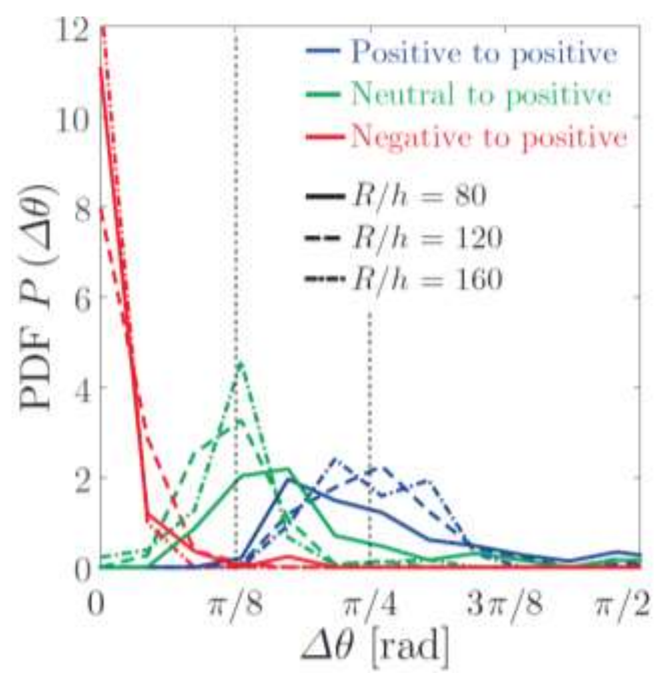

GLOBAL STRUCTURE IN TORUS

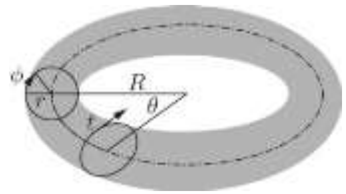

Global orientation of the crystal lattice:

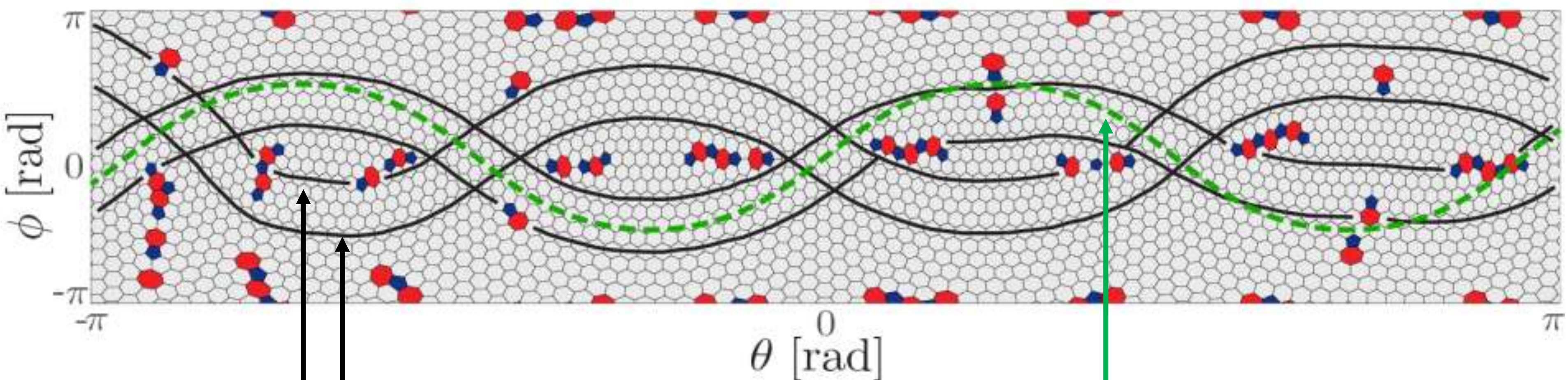

Lines connecting
consecutive lattice lements

Geodesic of minimum
Gaussian curvature

Hypothesis:
Nucleation of regular (hexagonal) lattice is favored
along lines with minimum Gaussian curvature.

PRE-STRETCH INDUCED PATTERNS

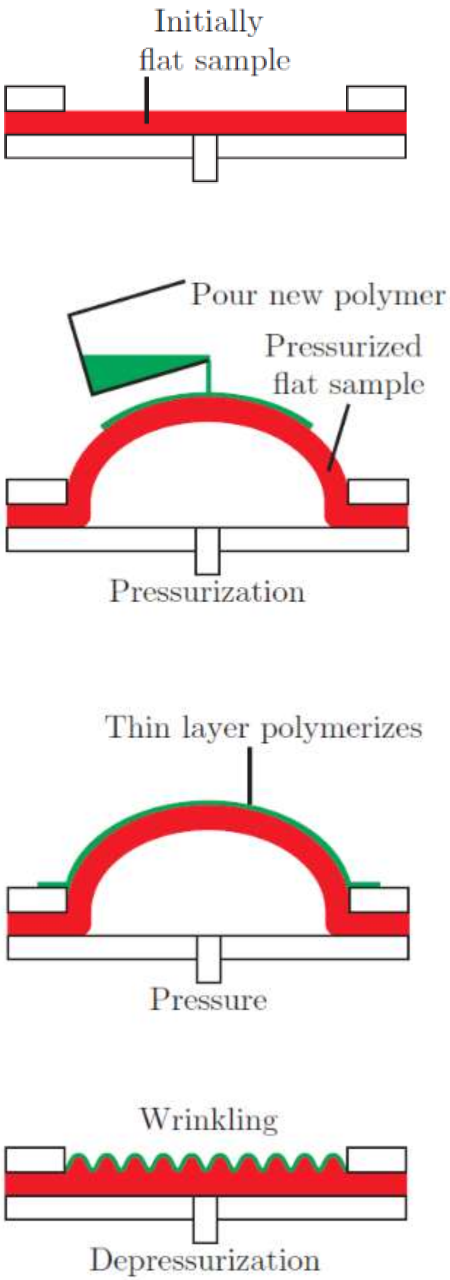

New method to create different patterns:

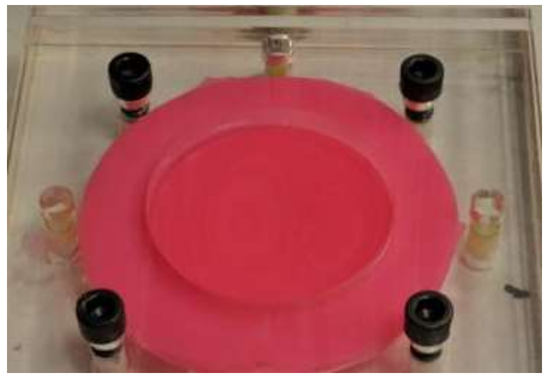

VPS8 – E ≅ 0.22 MPa

$\lambda_x = \lambda_y \cong 2$

VPS32 – E ≅ 1.2 MPa

Thickness ≅ 300 μm

PRE-STRETCH INDUCED PATTERNS

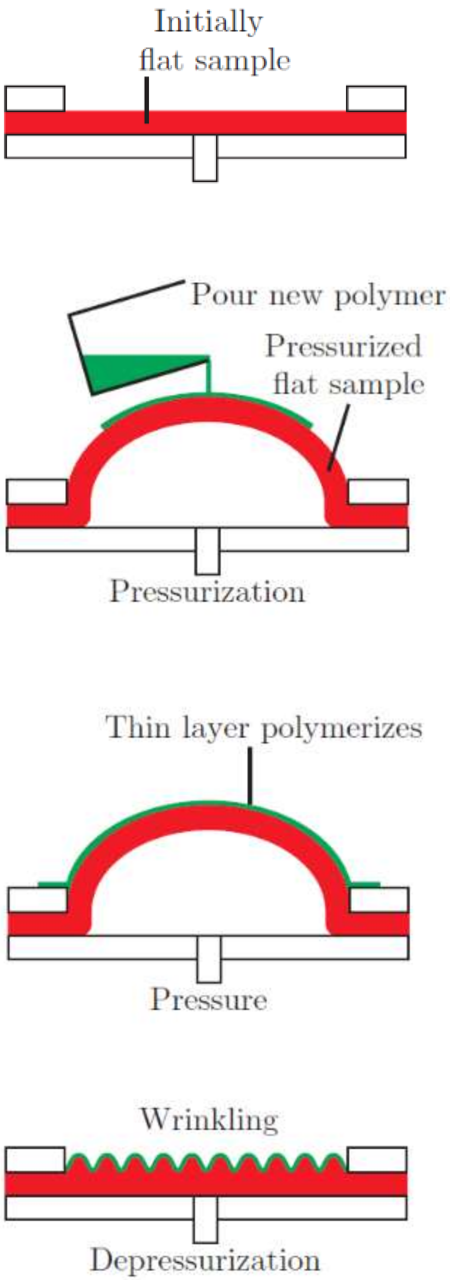

New method to create different patterns:

PRE-STRETCH INDUCED PATTERNS

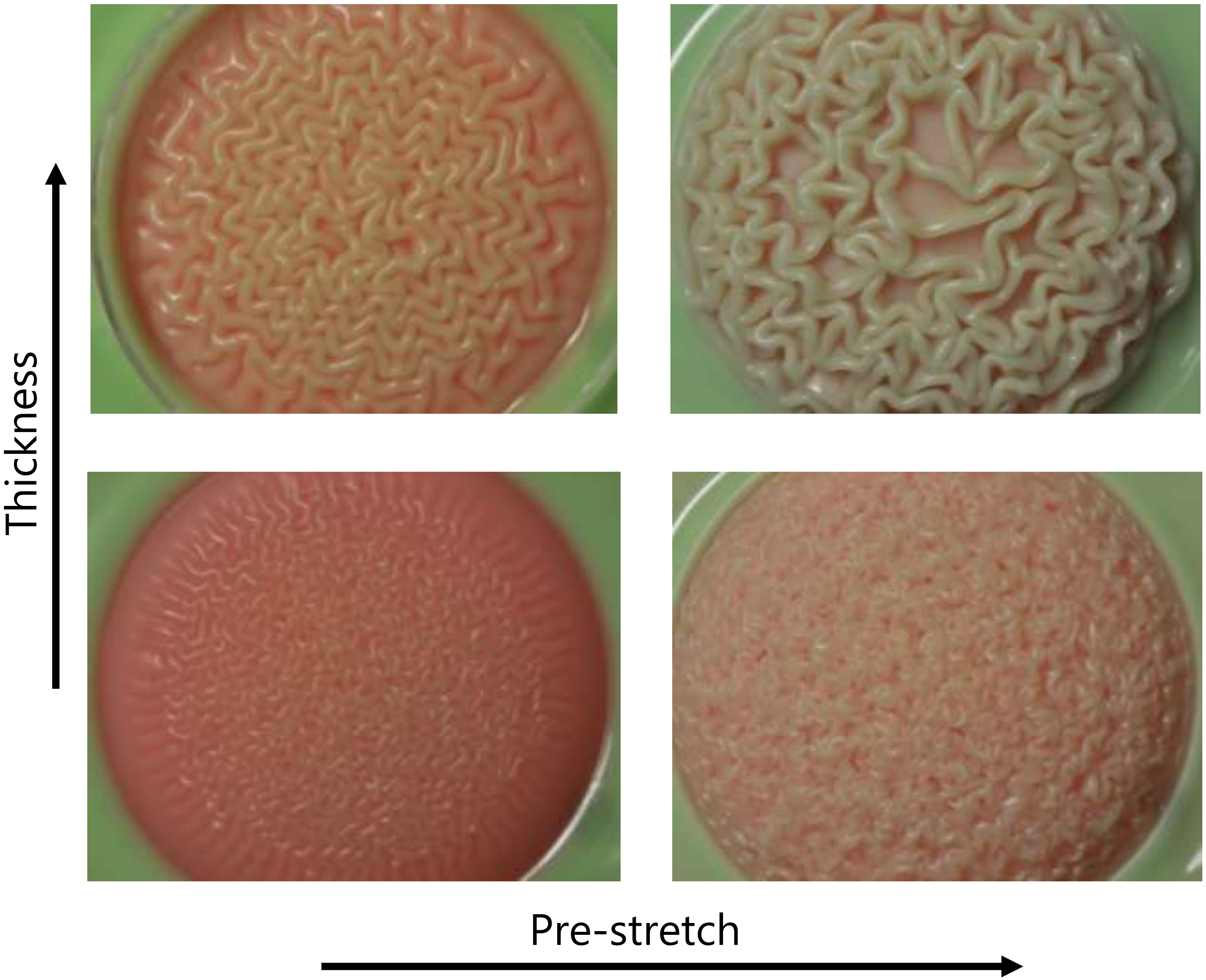

The ridges are fully bonded.

Different from telephone chord instability.

PRE-STRETCH INDUCED PATTERNS

Test with same material as substrate and thin film.

The wrinkles appear even with no stiffness mismatch.

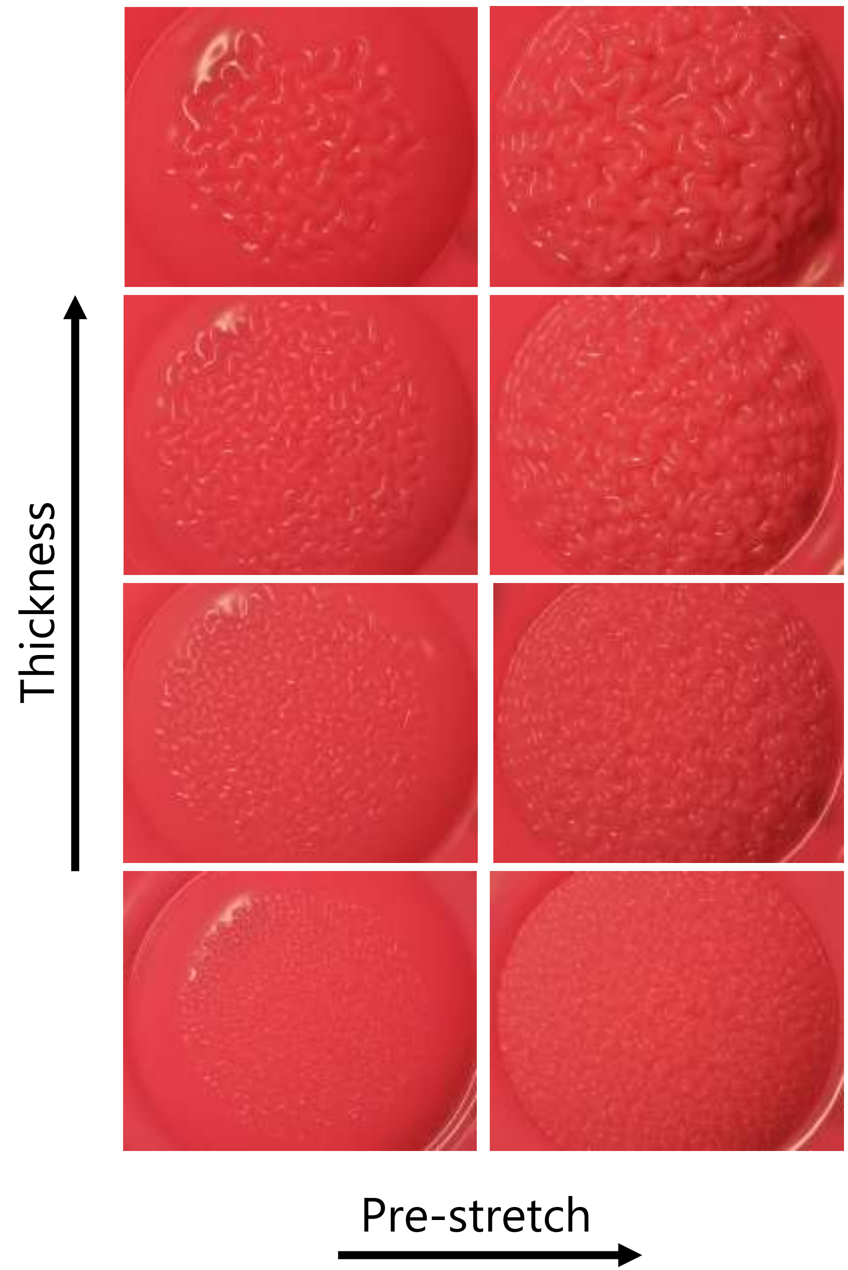

PRE-STRETCH INDUCED PATTERNS

Self-organized patterns:

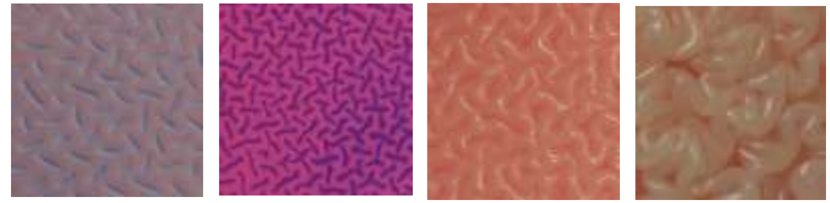

Model to study patterns in biological systems:

Pres-stretch

Differential growth

Extend known phase-diagram to biaxial loading:

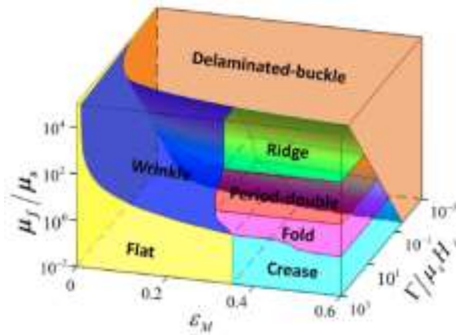

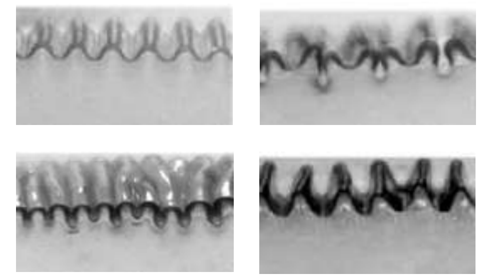

Wang and Zhao (2015)

Applications:

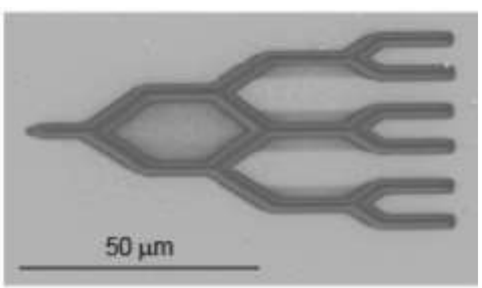

Microfluidics
(Moon et al., 2009)

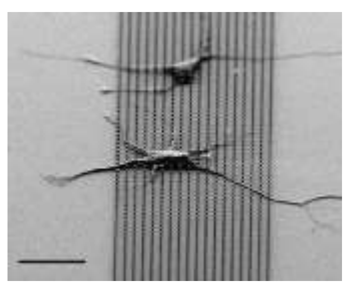

Cellular adhesion
(Craighead et al., 2001)

Folding pattern
(Tachi, 2015)

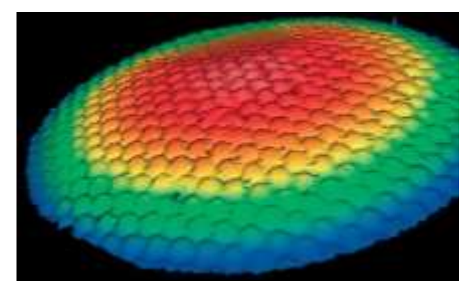

Micro lenses
(Chand and Crosby, 2006)

MATERIALS FOR OPTICAL ATTENUATION

Pure PDMS

PDMS + dye

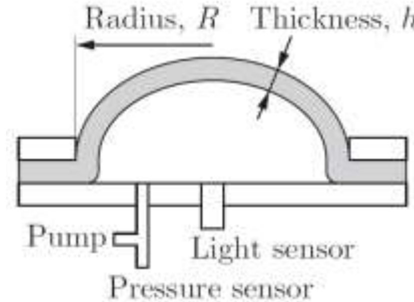

Optical attenuation changes as the system is stretched:

FLJ, Kumar and Reis, *Adv. Opt. Mat.*, 2016

MATERIALS FOR OPTICAL ATTENUATION

Attenuation as function of stretch:

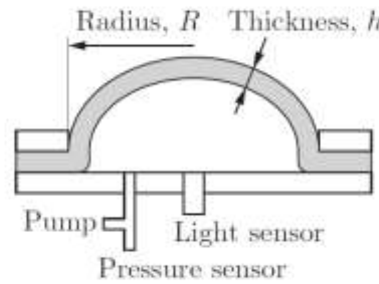

Beer-Lambert law: $T = 10^{-\varepsilon c t}$

3D elasticity: $t = t_0 \lambda$

$\Rightarrow T = T_0^{-\lambda}$

Repeatable and fast:

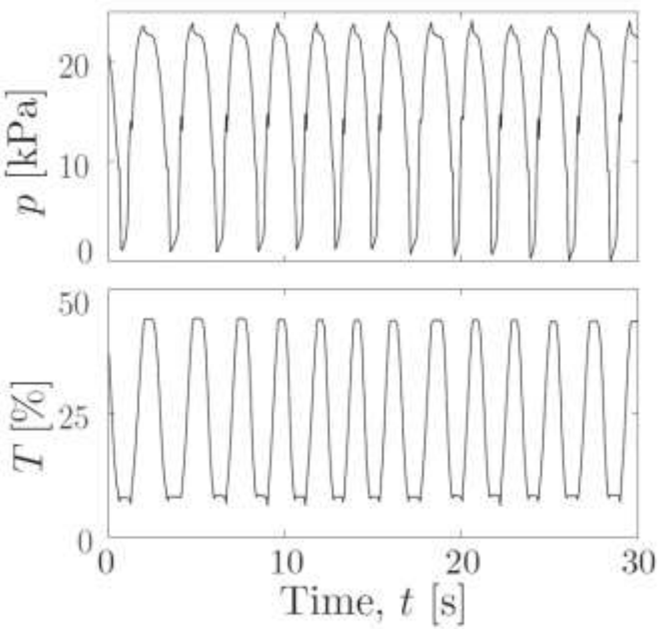

Predictable:

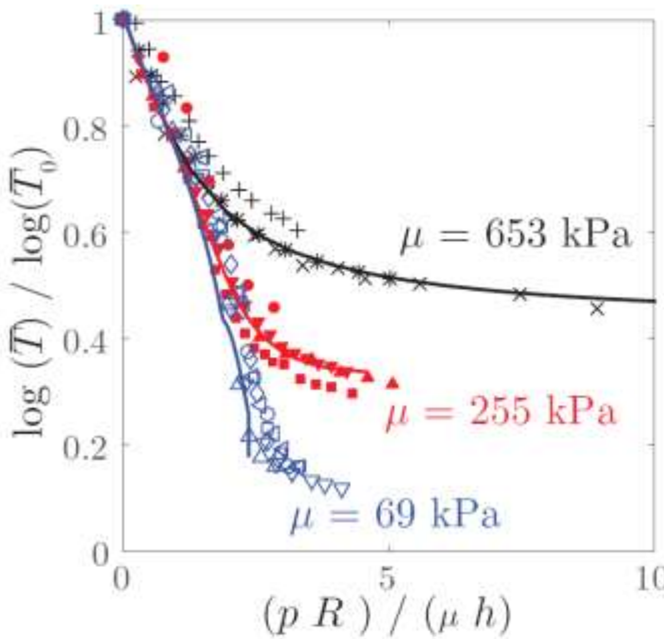

MATERIALS FOR OPTICAL ATTENUATION

Color dye for band-pass behavior:

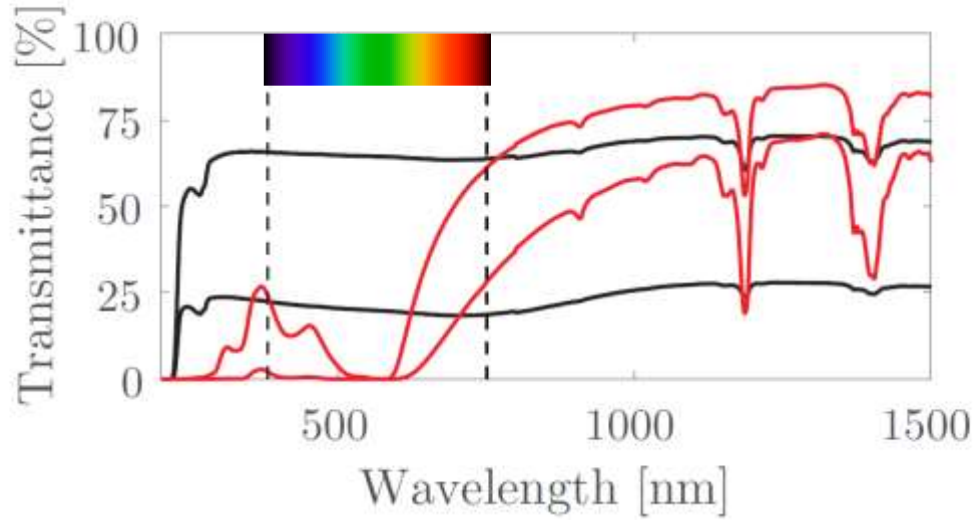

Surface topography to increase effect:

SUMMARY AND PERSPECTIVE

Materials with engineered microstructure **+** **Nonlinear mechanics of soft and flexible structures**

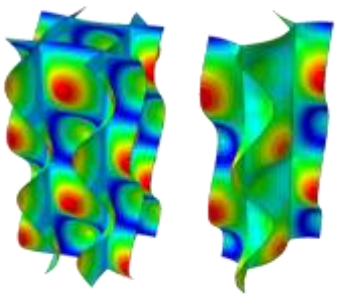

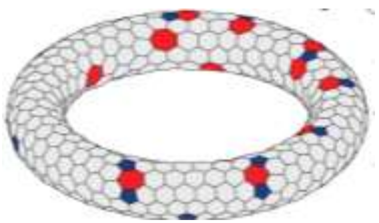

Overall strategy:

Combination of experiments with analytical and numerical work.

Simplified experiments → Modeling → Realistic experiments

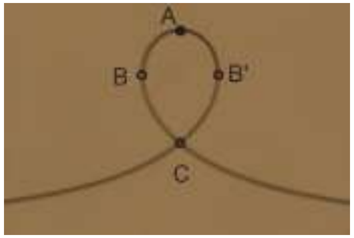

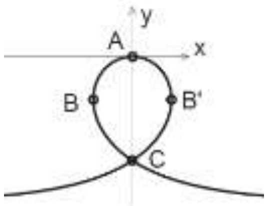

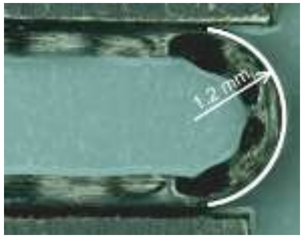

Flexible composites

Fiber microbuckling allows high curvatures

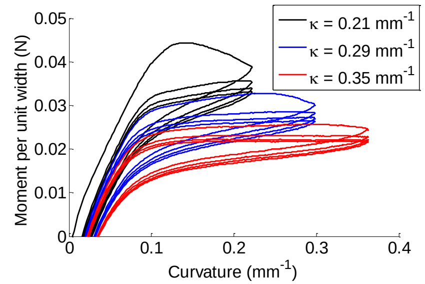

Nonlinear behavior and strain softening

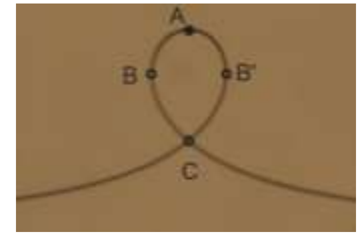

Predict failure of fibers in the appropriate geometry

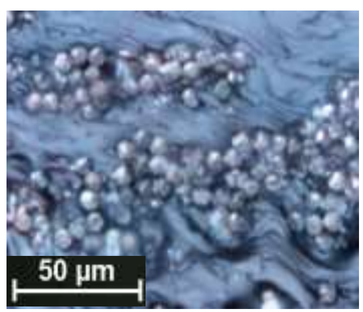

Real fiber microstructure

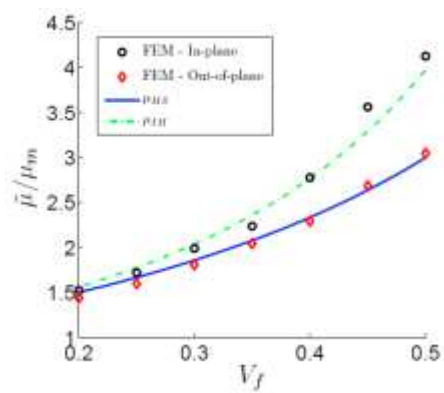

Response depends on deformation mode

Patterns on soft solids

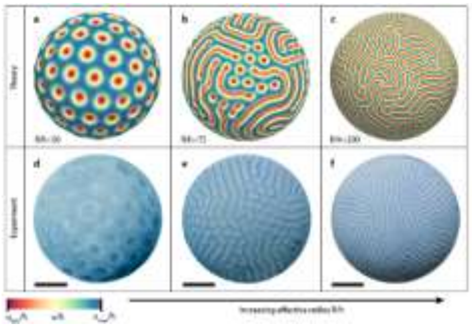

Curvature influences wrinkling patterns

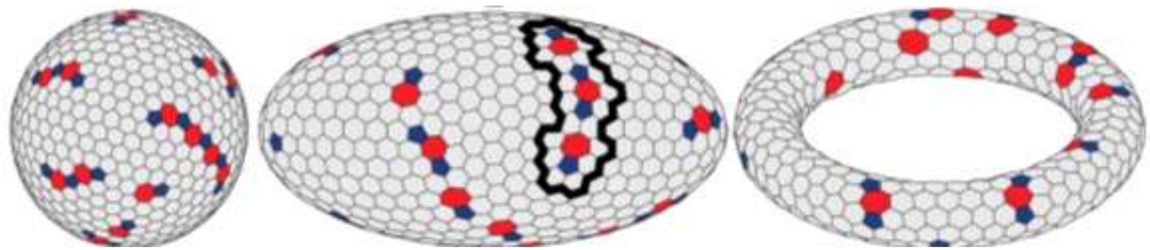

Model used to study the effect of Gaussian and principal curvatures

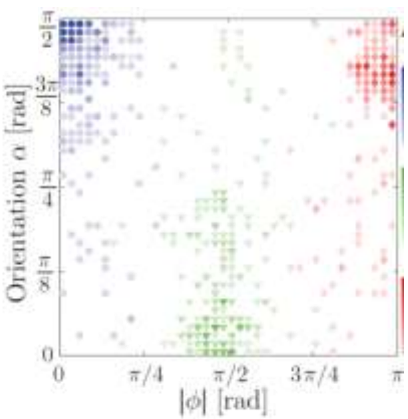

Curvature gradient controls defects

New patterns available through pre-stretching

Material for tunable opacity

Engineered microstructure + Soft and flexible structures

Fundamental problems:

- Instabilities
- Failure/damage
- Microstructure
- Homogenization
- Patterns
- Actuation

Applications:

Deployable structures

Maqueda et al. (2012)

Draping of textiles

amtcomposites

Soft robotics

Whitesides group

Solar sails

University of Surrey

Biomedical devices

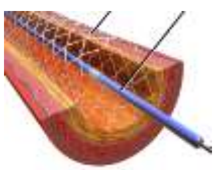

Active mirrors

Patterson et al. (2012)

Cell characterization

Beningo et al. (2002)

Flexible electronics

Rogers et al. (2010)

THANK YOU

Funding:

Keck Institute for Space Studies

NASA

SAINT-GOBAIN

MIT&MI MIT and Masdar Institute Cooperative Program

BACK UP SLIDES

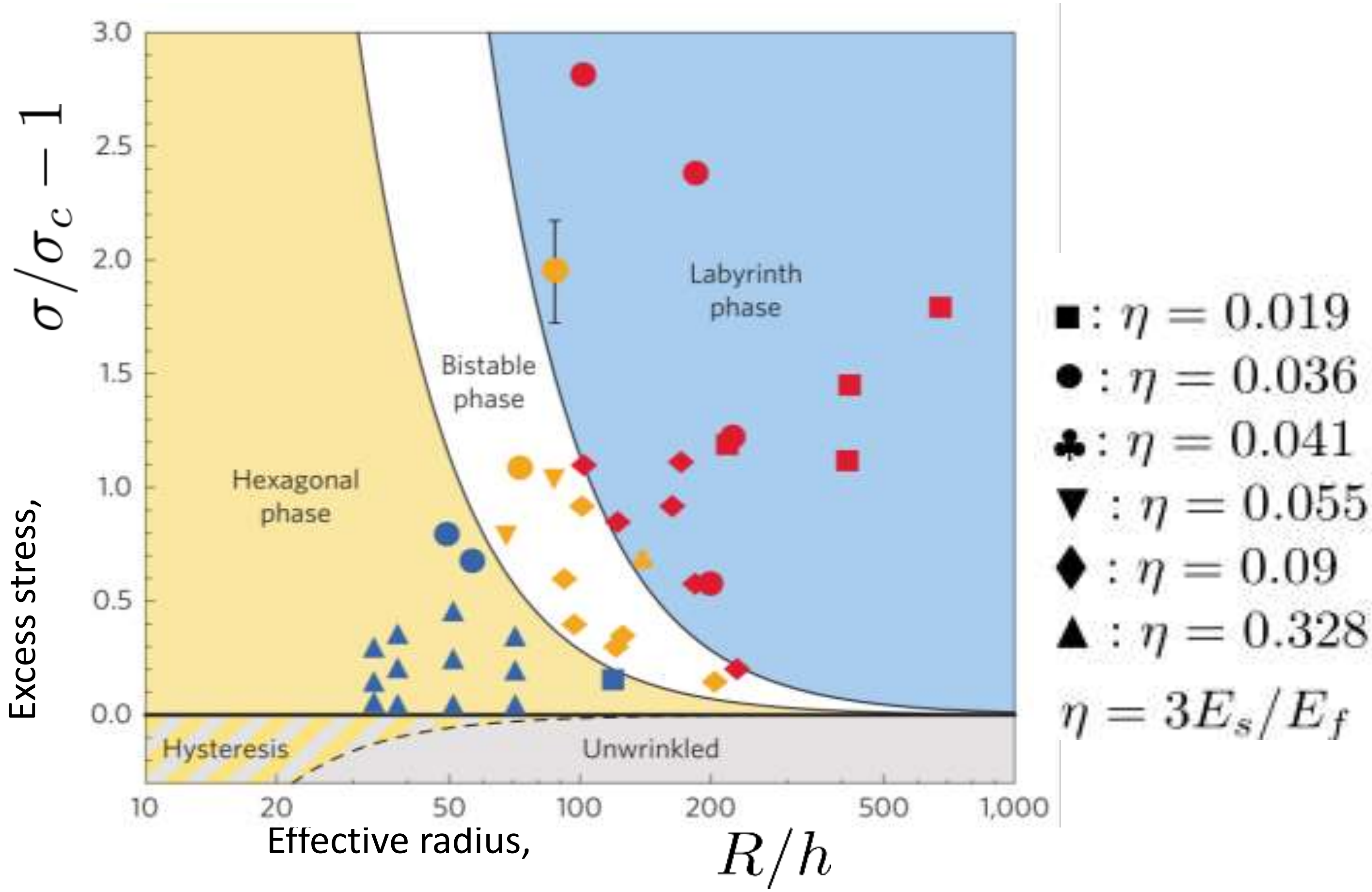

3.0
2.5
2.0
1.5
1.0
0.5
0.0
Excess stress, $\sigma/\sigma_c - 1$
Labyrinth phase
Bistable phase
Hexagonal phase
Hysteresis
Unwrinkled
10
20
50
100
200
500
1,000
Effective radius, R/h
■ : $\eta = 0.019$
● : $\eta = 0.036$
♣ : $\eta = 0.041$
▼ : $\eta = 0.055$
♦ : $\eta = 0.09$
▲ : $\eta = 0.328$
$\eta = 3E_s/E_f$

MOTIVATION AND BACKGROUND

Mode selection

Energy minimization

Observed experimentally

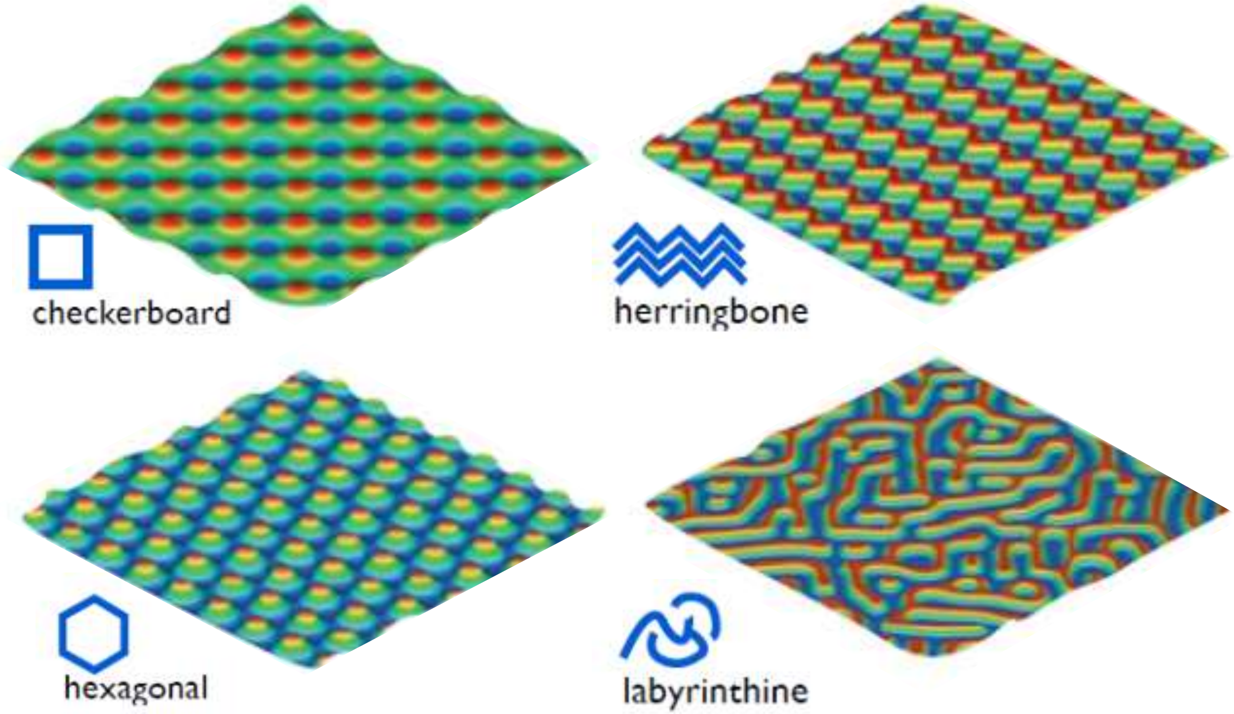

Audoly and Boudaoud (2008)
Cai et al. (2011)

Slight initial curvature may play an important role in mode selection.

Can we model its effect?

DEFECTS IN GRANULAR CRYSTALS

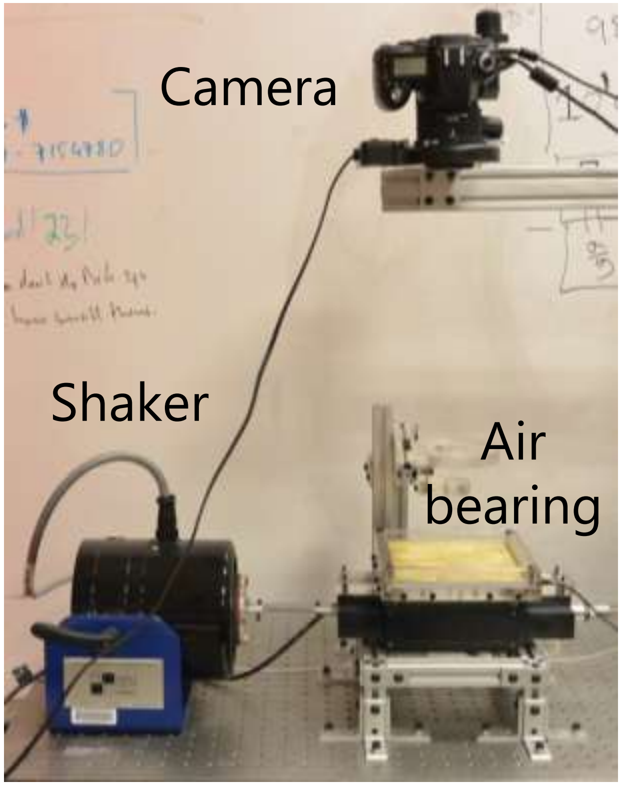

Time evolution of defect
under horizontal vibration

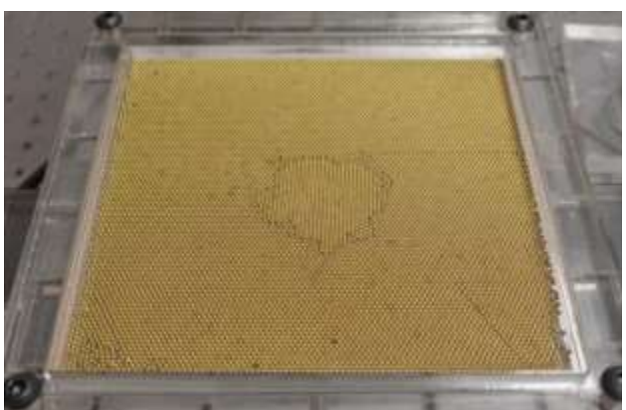

Defect ~ 450-500 particles
Imaging ~ 0.7 Hz   Video 25x speed
f = 28 Hz   A = 0.23 mm   a = 30 m/s^2

Horizontal tray (147x147 mm)
9400 monodisperse brass spheres
d = 1.5875 ± 0.0025 mm (1/16″ grade 200)

DEFECTS IN GRANULAR CRYSTALS

Crystal – Defect – Boundary

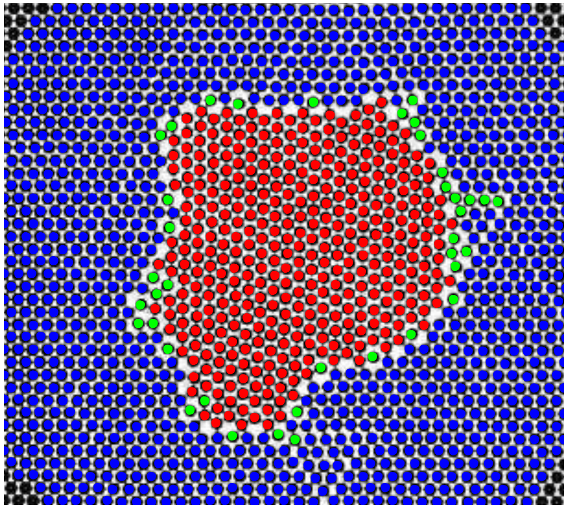

Structure on boundary correlates with misorientation

High (25-30º)

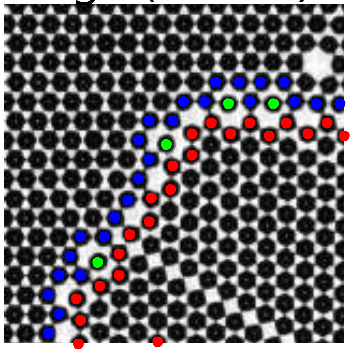

Coincident lattice

Medium (15-20º)

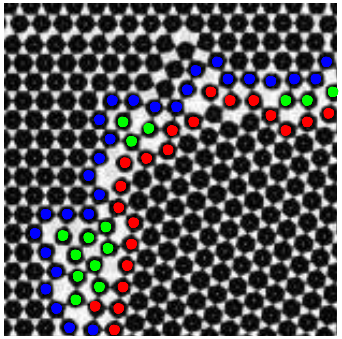

Glassy region

Low (5-10º)

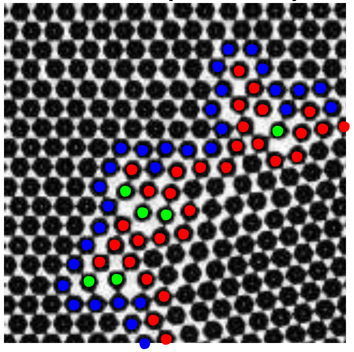

Dislocations

Local Voronoi density:

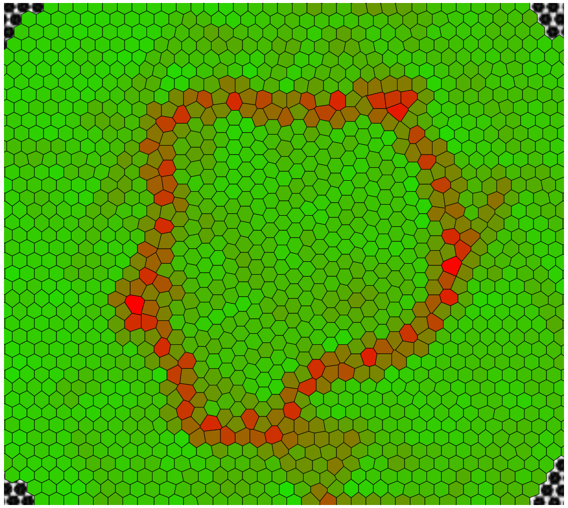

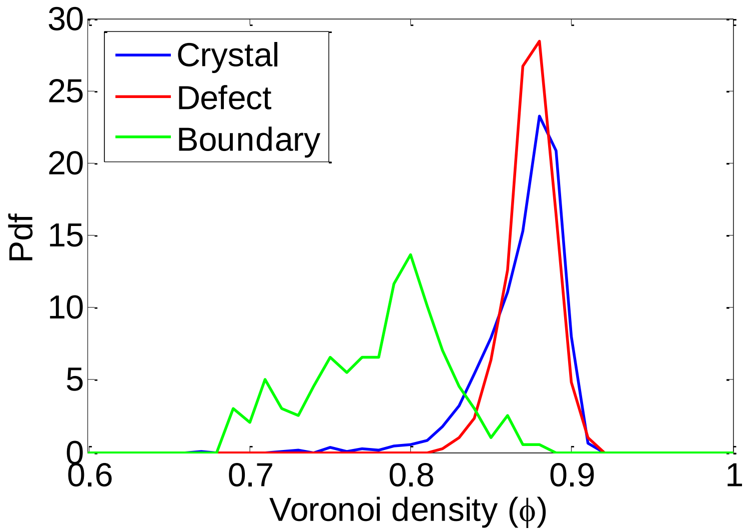

High spread in healing time.

Next step: high speed camera to measure “temperature”.

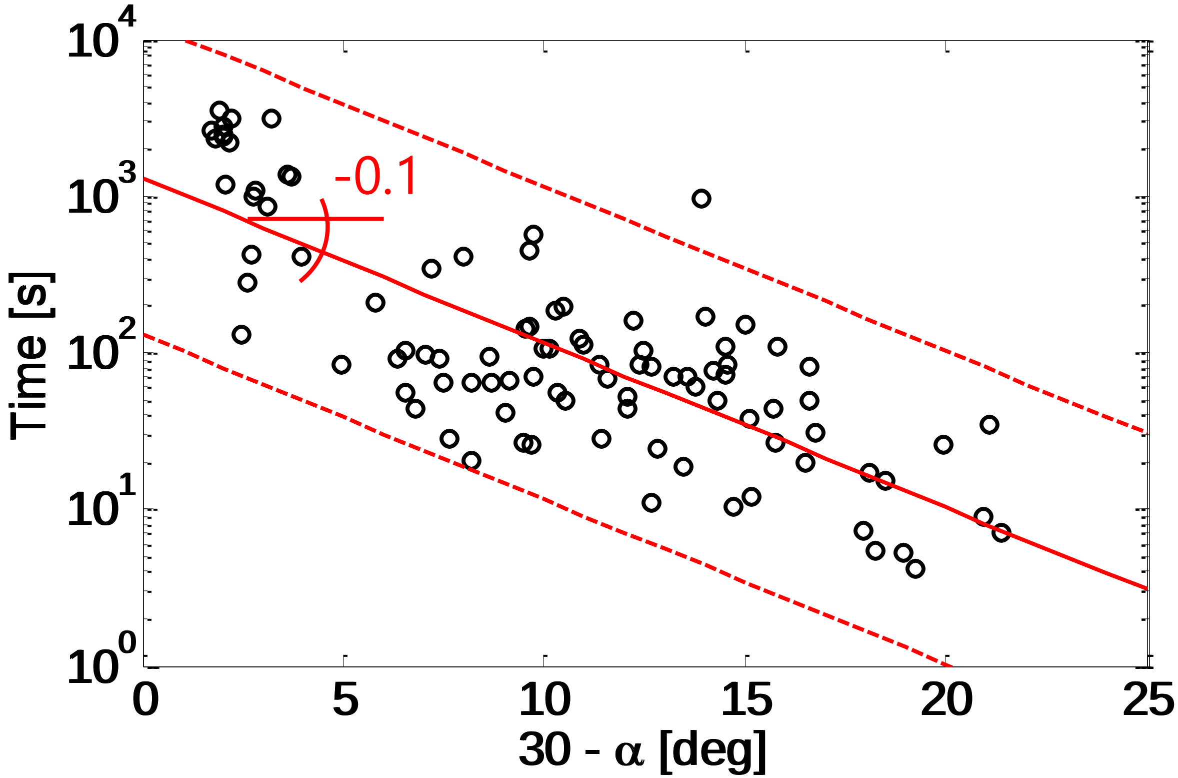

$$T = T_0 e^{k\alpha}$$

$$k = -0.24 \pm 0.04 \quad [1/\mathrm{deg}]$$

$$T_0 = 1295^{+732}_{-467} \quad [\mathrm{s}]$$

Goal:

Model system to study the dynamics of grain boundaries in general crystalline media.

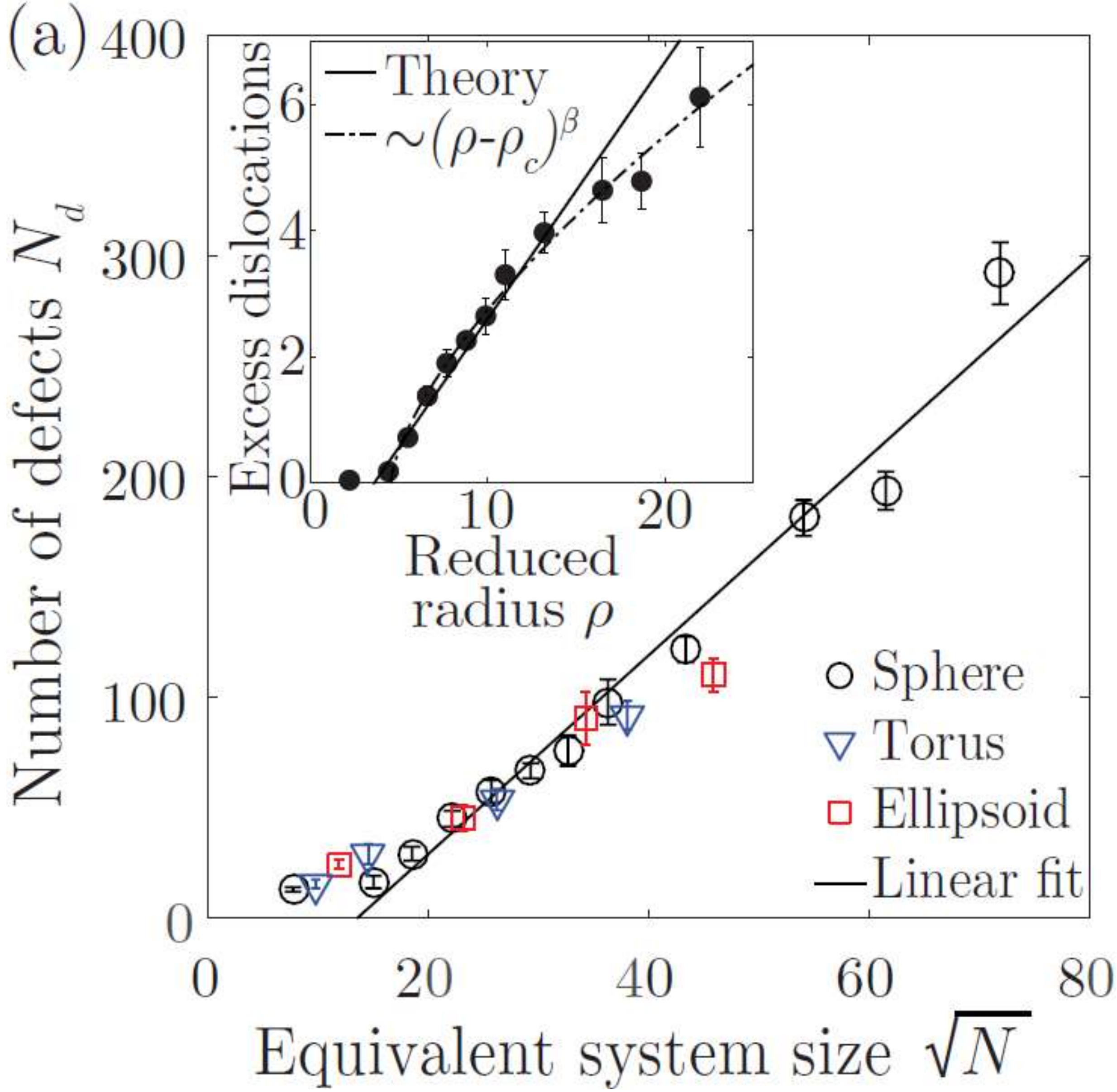

(a)
Number of defects N_d
Equivalent system size $\sqrt{N}$
0
100
200
300
400
0
20
40
60
80
Sphere
Torus
Ellipsoid
Linear fit
Theory
$\sim(\rho\text{-}\rho_c)^\beta$
Excess dislocations
Reduced radius ρ
0
2
4
6
0
10
20

HOMOGENIZATION

Implicit assumption: isotropy of the RVE.

Is the response the same for all loading directions?

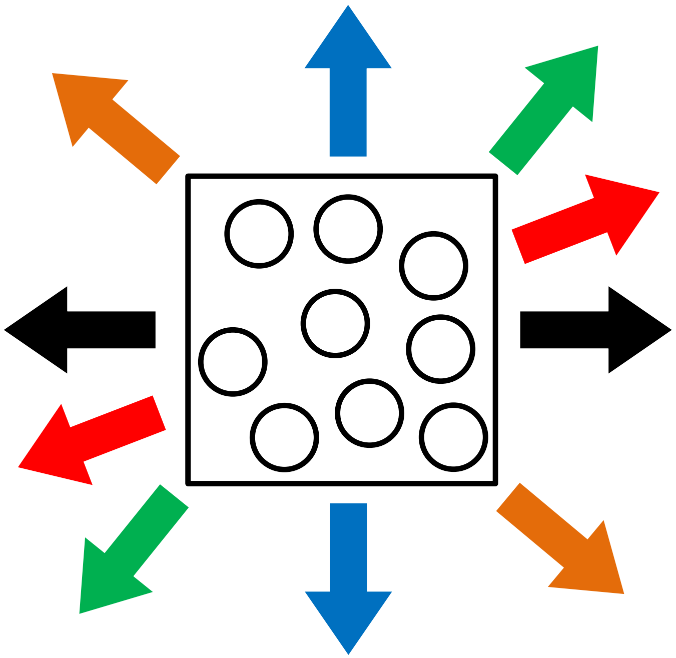

Principal stretches: $\lambda_1 \;,\; \lambda_2 \;,\; \lambda_3$

Incompressibility: $\lambda_1\,\lambda_2\,\lambda_3 = 1$

Plane strain: $\lambda_2 = 1$

Spectral theorem: $\mathbf{C} = \sum_{1}^{3} \lambda_i \mathbf{n_i} \otimes \mathbf{n_i}$

All deformations can be described by stretch and direction:

$\lambda_1 = \lambda$ $\qquad$ $\lambda_2 = 1$ $\qquad$ $\lambda_3 = 1/\lambda$

$\mathbf{n_1} = [0 \;\; \cos\theta \;\; \sin\theta]$ $\qquad$ $\mathbf{n_2} = [1 \;\; 0 \;\; 0]$ $\qquad$ $\mathbf{n_3} = [0 \;\; -\sin\theta \;\; \cos\theta]$

HOMOGENIZATION

Ten different realizations of the RVE.

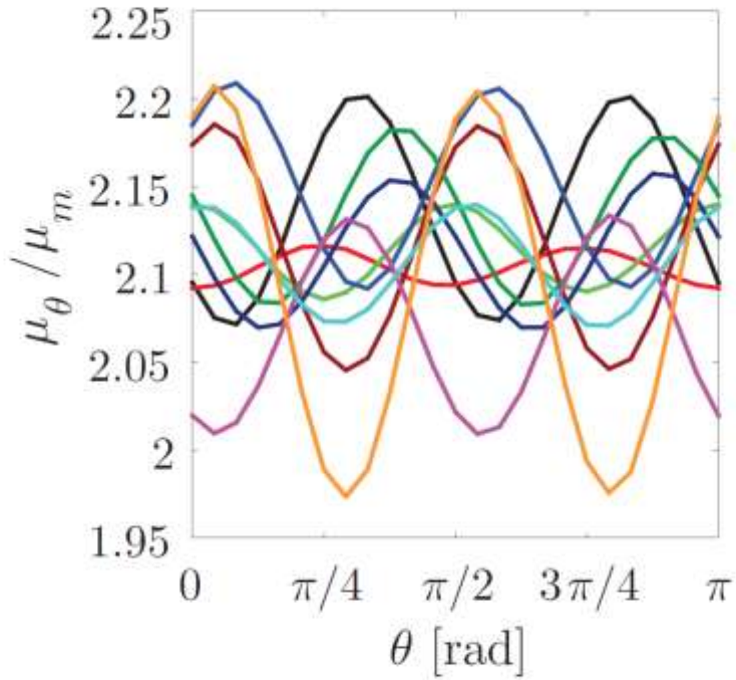

Response is a sine:

$$\mu_\theta = \tilde{\mu} + \Delta\mu \sin\left(4\theta + \theta_0\right)$$

Parameters change for each RVE.

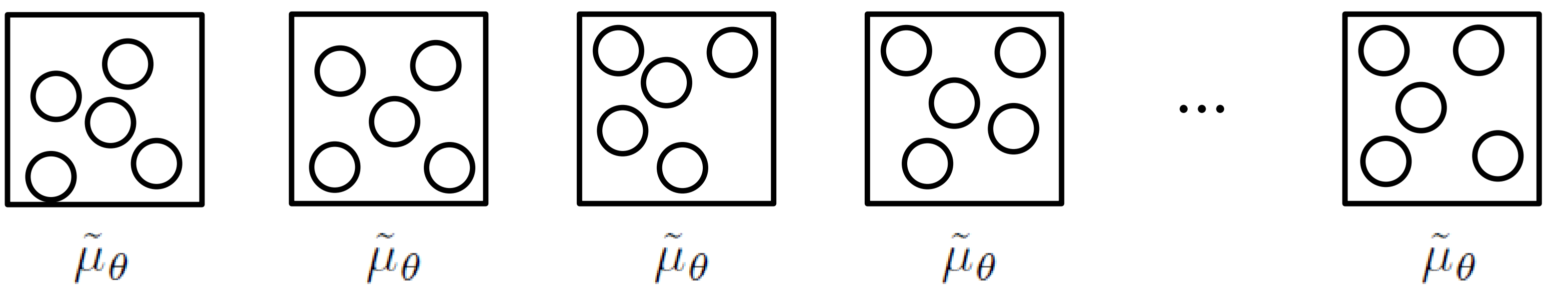

Expected value: $E_{RVE}[\tilde{\mu}_\theta]$

Coefficient of variation: $CV_{RVE}[\tilde{\mu}_\theta] = STD_{RVE}[\tilde{\mu}_\theta] / E_{RVE}[\tilde{\mu}_\theta]$

HOMOGENIZATION

Considering all directions reduces variability between models and improves convergence in response.

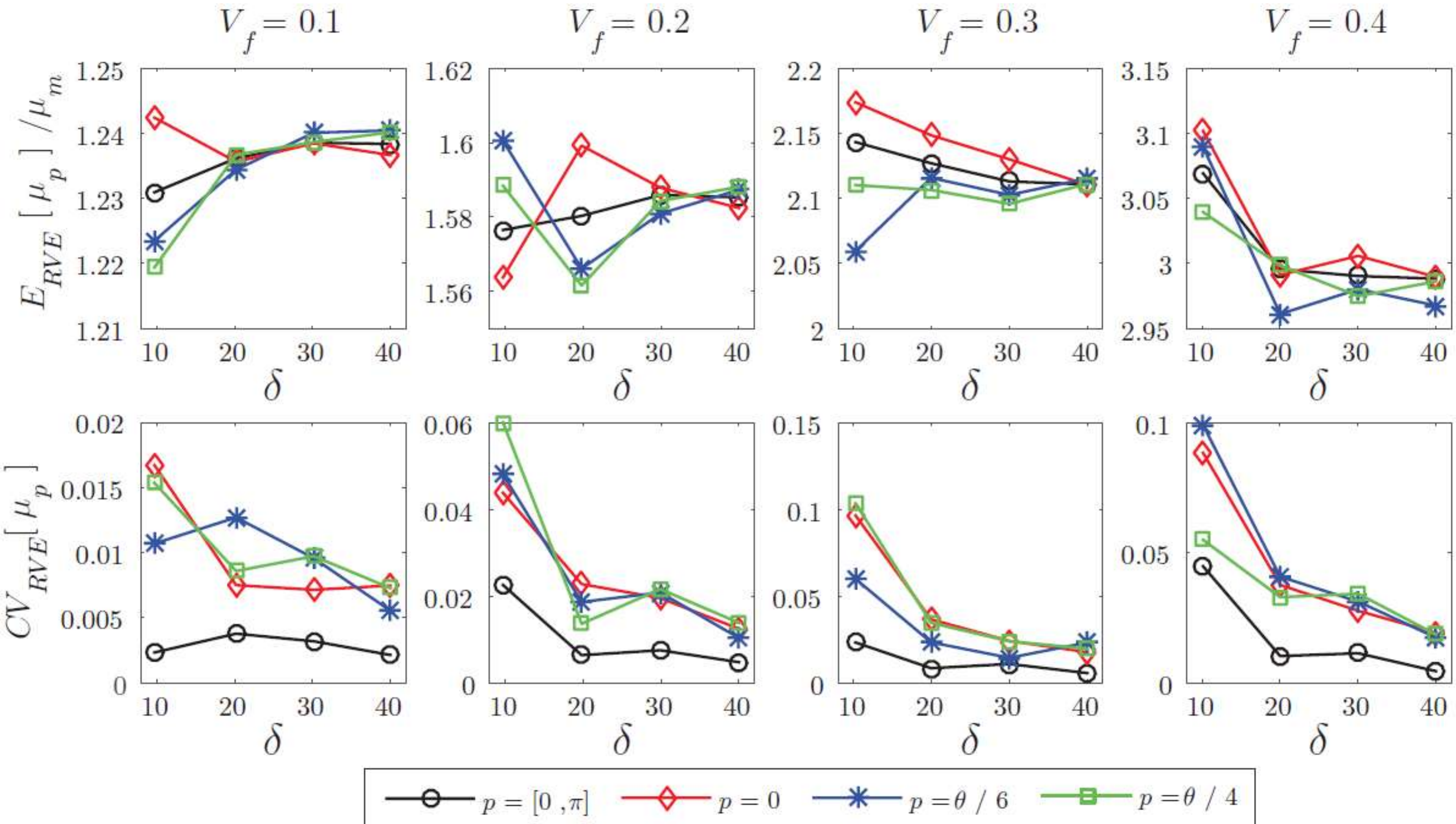

δ = L / R

FLJ, Composites B, 2016

ONGOING WORK

Fiber-matrix interphase (with Prof. Lopez-Pamies)

Effect of thin layer of material between fiber and matrix.

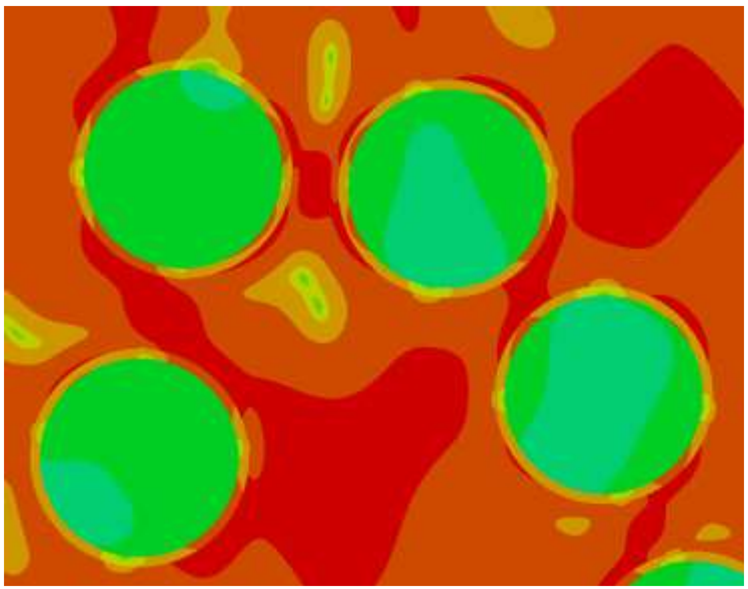

Homogenized response including damage

Introduce strain softening and damage into homogenized response.

Numerically efficient homogenization

Reduce the cost of numerical homogenization, taking into account:

- RVE anisotropy
- Range of fiber interaction.